THE ARIZONA PHYSIOLOGICAL SOCIETY

November 13-14, 2015

Midwestern University - Glendale

Sponsored by:

The American Physiological Society
Midwestern University, Department of Physiology & Office of the President
University of Arizona Departments of Physiology & COM -Tucson
Northern Arizona University
Arizona State University

ADI
DMT
VWR
Fisher Scientific

AzPS 8th Annual Meeting

Midwestern University
Glendale, Arizona

Program

Friday November 13th

12.00-5.00 Registration in Lobby- Cholla Building.
12.00-1.30 Set up Friday's Posters (all 28 Graduate students) in Cholla: Rooms 112-114

1.30-1.45 **Welcome to the Meeting** –Kiisa Nishikawa, PhD, President, AzPS.

1.45-3.00 **Session I, Cholla C: "Trainee Physiology Research Presentations"**
Chairs: Tobias Riede, PhD. Assistant Professor, (MWU) &
Johnnie Moore-Dotson, PhD. Post-doctoral fellow (UA-Tuc).

1.45-2.00 **T1. Philip Sandoval**, Graduate Student, UA-Tuc (Mentor: Dr. S. Wright). "The kinetics of ligand interactions with the organic cation NBD-MTMA at OCT2."
2.00-2.15 **T2. Andrew D'Lugos,** Graduate Student, ASU (Mentor: Dr. J. Dickinson). "High intensity exercise preserves myocellular size throughout doxorubicin treatment."
2.15- 2.30 **T3. Dennis Pollow Jr.**, Graduate Student, UA-Tuc (Mentor: Dr. H. Brooks). "FOXP3+ regulatory T cell depletion eliminates ANGII-induced hypertension resistance in female mice."
2.30-2.45 **T4. Meli'sa Crawford**, Graduate Student, ASU (Mentor: Dr. K. Sweazea). "In the short term, poor nutrition promotes simple steatosis without inflammation in adolescent rats."
2.45-3.00 **T5. Anthony Hessel**, Graduate Student, NAU (Mentor: Dr. K. Nishikawa). "An evaluation of eccentric contraction function during a stretch shortening cycle for muscles in mice."

3.00-3.15 **Break** - Coffee

3.15-4.30 **Session II, Cholla C or Mesquite Hall:**
"Sim lab & teaching health care professionals":
Layla Al-Nakkash, PhD, Professor (MWU) & Jaqueline Spiegel, MS, PA-C (MWU), Director Clinical skills and Simulation Center (MWU).
or
Session II: "Physiology Outreach"
Karen Sweazea, PhD. Associate Professor (ASU) & Cindy Rankin, PhD. Associate Professor (UA-Tuc).

Following a brief talk by Sim. Director, Jacqueline Spiegel and Layla Al-Nakkash, attendees will rotate through the Sim lab to watch a clinical demo, or attend the Outreach Talk/demos and swap half way through. ~30 min each.

4.30-4.45 **Break**

4.45 - 5.30 **Session II, Cholla C: "Trainee Physiology Research Presentations"**
Chairs: Tom Broderick, PhD. Professor, (MWU) &
Megan Garlapow, PhD. Post-doctoral fellow (ASU).

4.45-5.00 **T6. Christine Gibson**, Graduate/MS-II Student, MWU (Mentor: Dr. M Esfandiarei). "Mild aerobic exercise improves aortic wall integrity and elasticity in a mouse model of Marfan syndrome."

5.00-5.15 **T7. Christine Hernandez**, Graduate/CVM-II Student/, MWU (Mentor: Dr. T. Riede). "Experience-dependent changes in vocal production in male rats."

5.15-5.30 **T8. Faisal Masood**, Graduate/MS-II Student, MWU (Mentor: Dr. L. Al-Nakkash). "A mouse model of diabetes: loss of CFTR expression contributes towards reduced jejunum chloride secretion."

5.30- 6.30 **The AzPS Keynote Lecturer, Cholla C:** Dr. Andrew Biewener
Introduction: Kiisa Nishikawa, Ph.D. Regents Professor (NAU)

Andrew Biewener, Ph.D. Lyman Professor of Biology, Director Concord Station, Department of Organismic & Evolutionary Biology, Harvard University. **"How Do Running Animals Achieve Stability? The Neuromechanical Control of Rapid Locomotion"**	

6.30-7.30 **Chapter Reception & Buffet Dinner – Cholla 116-118**

7.30-8.00 **Minute Poster I - Cholla C** (All 28 Graduate student posters)
Chairs: Scott Boitano, Ph.D. Associate Professor (UA-Tuc), &
Christiane Danilo, Ph.D. Post-doctoral Fellow (UA-Tuc).

8.00-9.30 **Poster Presentations (28 posters)** - Cholla Rooms 112-114
All 28 Graduate Student posters

Saturday November 14th

8.00-9.00 Breakfast/poster setup (All regular, post-doc and undergrad posters)
8.00-9.00 Post-doctoral fellows invited to have breakfast with Dr. Biewener

9.00-10.30 **Session III, Cholla C: "Trainee Physiology Research Presentations"**
Chairs: Tom Broderick, PhD. Professor, (MWU) &
Christiane Danillo, PhD. Post-doctoral fellow (UA-Tuc).

9.00-9.15 **T9. James Sargent**, Undergraduate Student, ASU (Mentor: Dr. J. Harrison). "Age-related decline of anoxia tolerance in adult *drosophila melanogaster*."

9.15-9.30 **T10. Colleen Kerrigan,** Undergraduate Student, UA-Phx (Mentor: Dr. R. Gonzales). "Temporal expression of cyclooxygenase-2 following lateral fluid percussion injury in the male rat brain."

9.30-9.45 **T11. RussL Altabtabaee**, Undergraduate Student, ASU/MWU (Mentor: Dr. L. Al-Nakkash). "Effects of genistein diet on diabetic jejunum function and histology in the ob/ob mouse."

9.45-10.00 **T12. Brittney McCormick**, Undergraduate Student, UA-Phx (Mentor: Dr. T. Hale). "Differential cardiovascular and penile responses to angiotensin II and bradykinin B1-receptor antagonism treatment in Sprague-Dawley rats."

10.30-10.45 **Break**

10.45- 11.45 **The Arizona Distinguished Lecturer: Cholla C**
Introduction: Stan Lindstedt, Ph.D. Emeritus Professor (NAU).

Eldon Braun, Ph.D. Professor Emeritus
Department of Physiology
University of Arizona-Tucson

"The Comparative Physiology of Osmoregulation: Lessons from Avian Studies"

11.45-12.15 **Minute Poster II – Cholla C** (23 posters)
All 7 Post-doctoral Posters, all 11 Undergraduate Posters, and all 5 Regular member posters
Chairs: Layla Al-Nakkash, PhD. Professor (MWU) &
Dennis Pollow, Jr, Graduate Student (UA-Tuc).

12.15-1.15 **Poster Presentations** in Cholla –Rooms 112-114
All 7 Post-doctoral Posters, all 11 Undergraduate Posters, and all 5 Regular member posters

1.15-2.00 **Lunch: Cholla 116-118**
Graduate Students invited to have lunch with Dr. Andrew Biewener.
Judges meet regarding poster awards.

2.00-3.00 **Session V, Cholla C: Physiology Research in Arizona**
Chairs: Steve Wright, Ph.D. Professor (UA-Tuc) &
Robert LeMoyne, Ph.D. Post-doctoral Fellow (NAU).

2.00- 2.15 **T13. Manal Zein-Hammoud,** Post-doctoral Fellow, UA-Phx (Mentor: Dr. P. Standley). "Myofascial release-induced wound healing in 3-dimensional bioengineered tendons: role for fibroblast proliferation and collagen secretion."

2.15-2.30 **T14. John Kanady**, Post-doctoral Fellow, UA-Tuc (Mentor: Dr. J. Burt). "A lymphedema-inducing mutation of CX47, R259C, alters growth pattern and CX43 processing in rat insulinoma cells."

2.30-2.45 **T15. Taben Hale,** PhD, Associate Professor (UA-Phx). "Sex differences in cardiovascular responses to stress in adult rats prenatally exposed to dexamethasone."

2.45-3.00 **T16. Jon Harrison,** PhD, Professor (ASU). "Body position effects on hemolymph and air distribution in insects."

3.00- 3.30 **Business meeting/awards** & adjourn

Local Hotel options- be sure to ask for a Midwestern rate:

1. **SPRINGHILL SUITES.**

   7810 W Bell Rd

   Glendale, AZ, 85308

   623-878-6666 (2.5 miles from campus -$179+tax)

2. **THUDERBIRD EXECUTIVE INN**

   15249 N 59th Ave

   602-978-7987 (3 miles from campus-$140+tax)

3. **COUNTRY INN & SUITES**

   20221 N 29th Ave

   623-879-9000 (4.5-miles from campus- $79+tax)

4. **DRURY INN & SUITES**

   2335 W Pinnacle Peak Rd

   623-879-8800 (4.8 miles from campus- $104+tax)

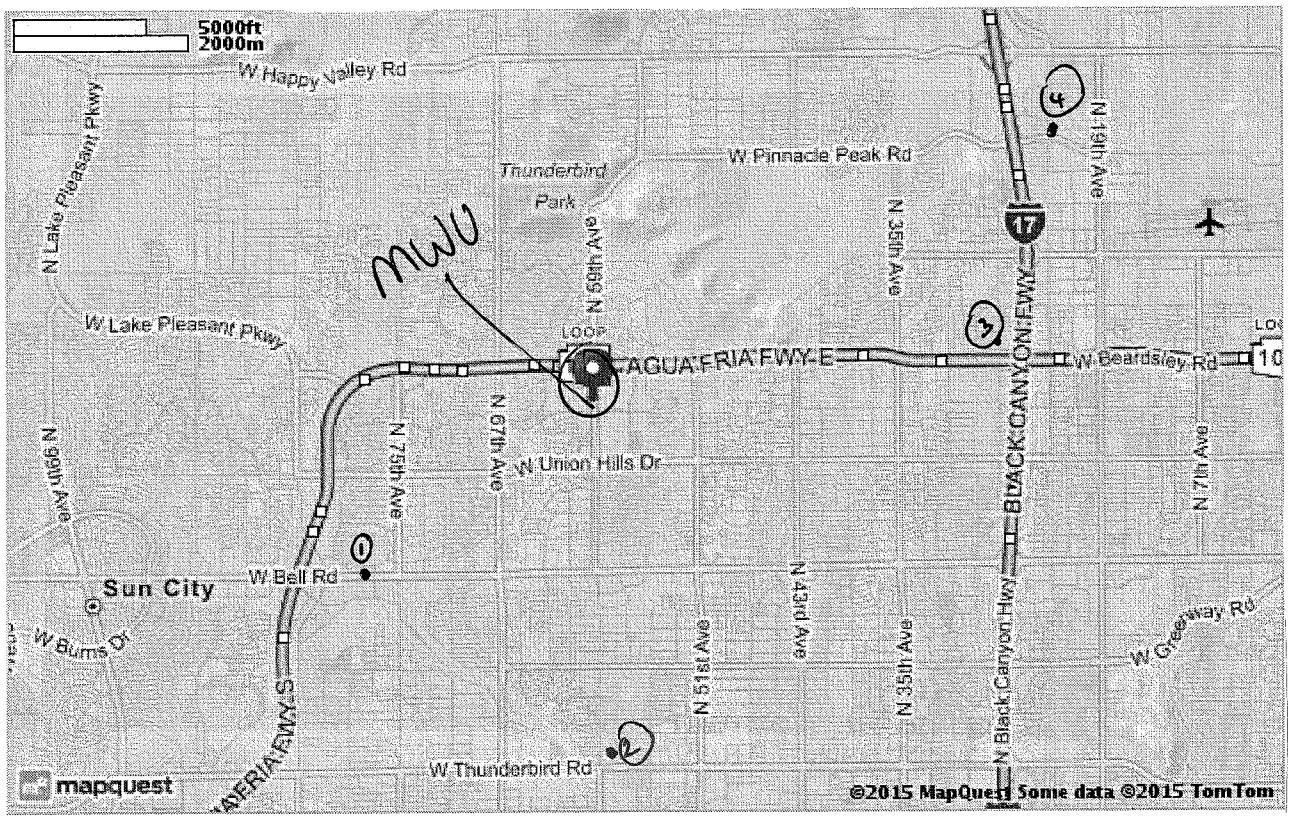

MIDWESTERN UNIVERSITY

GLENDALE, ARIZONA CAMPUS

1 Welcome Center
2 Welcome Center
3 Reflecting Pool
4 Sahuaro Hall
5 Ocotillo Hall
6 Cholla Hall
7 Agave Hall
8a Barrel Student Center I
8b Barrel Student Center II
8c Barrel Student Center III
9 Student Apartment Complex
10 Cactus Clubhouse
11 Foothills Science Center
12 Multispecialty Clinic
13 Eye Institute
14 Dental Institute
15 Companion Animal Clinic
16 University Administration
17 Glendale Hall
18 Mesquite Hall
19 Auditorium
20 Interfaith Chapel
21 Recreation and Wellness Hall
22 Cactus Wren Hall
P Parking

Directions to Midwestern University Glendale Campus (coming from Sky Harbor Airport)

Via Interstate 17

- Head north on Interstate 17
- Exit on Loop 101
- Continue west on 101 to 59th Avenue exit
- Turn left onto 59th Avenue
- Pass the Glendale Arrowhead Post Office; go through the light and take the next street left (Utopia)
- Midwestern University is on the left

Via Interstate 10

- Take Interstate 10 West to 101
- Take 101 North to 59th Avenue
- Turn right on 59th Avenue
- Pass the Glendale Arrowhead Post Office; go through the light and take the next street left (Utopia)
- Midwestern University is on the left

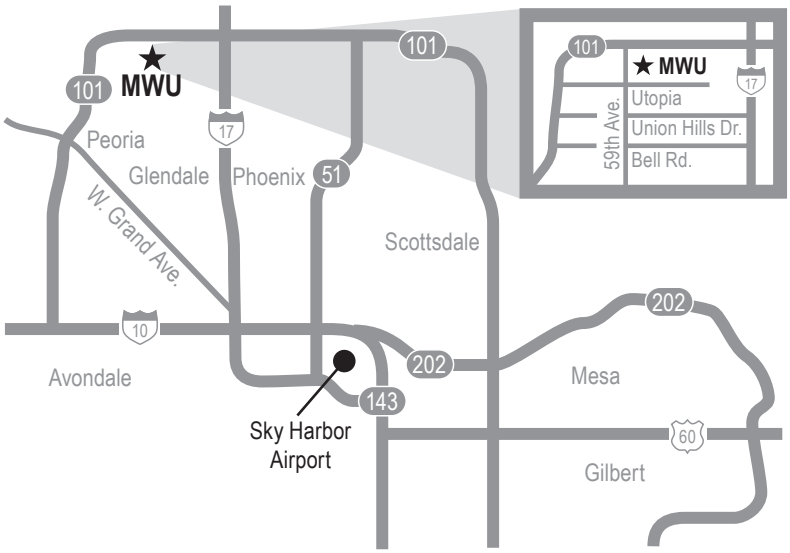

19555 North 59th Avenue • Glendale, AZ 85308 • 623.572.3215 • 888.247.9277 • www.midwestern.edu

Friday Posters, Arranged by Lead Author (alphabetical)

	Lead Author	Title
	GRADUATE STUDENTS	
F1	Wazir Abdullahi	TGF-β/ALK1 Signaling Alters Organic Anion Transporting Polypeptide 1a4 (Oatp1a4) Expression at the Blood-Brain Barrier
F2	Rifat Adity	The Effect of Prior Shortening on Residual Force Enhancement after Stretch in Mouse Muscles
F3	Matthew Bull	Mechanotransduction via Titin's N2B Element Contributes to Cardiac Remodeling
F4	Jacob Campbell	Metabolic and Genetic Implications of Survival in Anoxia
F5	Maura Cotter	Drug Discovery: Lipidation of Connexin Mimetic Peptides Increases Efficacy in Gap Junction Inhibition
F6	Meli'sa Crawford	In the Short Term, Poor Nutrition Promotes Simple Steatosis Without Inflammation in Adolescent Rats
F7	Samantha Day	CAPN10 and ADCY5 SNPs are associated with obesity-related phenotypes and DNA methylation in human skeletal muscle
F8	Andrew D'Lugos	High Intensity Exercise Preserves Myocellular Size Throughout Doxorubicin Treatment
F9	Michael Flood	Dopamine Modulates the Pre-Synaptic Unevoked Release of Glycine in the Inner Retina
F10	Christine Gibson #1	Evaluation of the Effects of Mild Aerobic Exercise on Aortic Contraction in a Mouse Model of Marfan Syndrome
F11	Christine Gibson #2	Mild Aerobic Exercise Improves Aortic Wall Integrity and Elasticity in a Mouse Model of Marfan Syndrome
F12	Jason Harmon	Caveolae as Potential Regulators of TGF-β and AT_1R Signaling in Aortic Smooth Muscle Cells
F13	Christine Hernandez	Experience-dependent changes in vocal production in male rats
F14	Anthony Hessel	An Evaluation of Eccentric Contraction Function during a Stretch Shortening Cycle for Muscles in Mice
F15	Nyssa Hoffman	Plasma Free Fatty Acid and Amino Acid Responses to Glucose-Induced Insulinemia in Insulin-Resistant Subjects
F16	Nicole Jacobsen	Gap Junction Channel Conductivity does not Predict Insulinoma Cell Proliferative Phenotypes Induced by Connexin 37 Phospho-Isoforms
F17	Gabriel Kelly	Integrin β4 mRNA splicing patterns are influenced by SNPs
F18	Katon Kras	The Enzyme Nagarse Improves Purity and Functional Coupling of Skeletal Muscle Subsarcolemmal Mitochondria Preparations
F19	Lakshmi Madhavpeddi	Angiotensin II Modulates Sex Steroid Metabolizing Enzyme and Receptor Expression in Cardiac Fibroblasts from Male and Female Rats

F20	Faisal Masood	A Mouse Model of Diabetes: Loss of CFTR Expression Contributes to Reduced Jejunum Chloride Secretion
F21	Michael Minicozzi	Are there Performance Tradeoffs in the Ability to Perform the Aquatic C-Start and Terrestrial Tail-Flip Jump?
F22	Carissa Miyano	Stretch Shortening Cycle Protocols Demonstrate the Age Associated Difference in Eccentric Properties of Edl And Soleus Muscles
F23	Dennis Pollow	FOXP3+ Regulatory T Cell Depletion Eliminates Ang II-induced Hypertension Resistance in Female Mice
F24	Puneet Raman	Palmitate-Induced Gylcosylation of Cyclooxygenase-2 in Primary Human Vascular Smooth Muscle Cells
F25	Jayachandran Ravichandran	Contrasting Processes to Measure Mitochondrial Function in Cultured Myotubes Versus Whole Muscle: Preliminary Studies
F26	Candy Rivas	Drug Discovery: Novel Protease Activated Receptor 2 Antagonists
F27	Philip Sandoval	The Kinetics of Ligand Interaction with the Organic Cation NBD-MTMA at OCT2
F28	Uzma Tahir	A Powered Ankle-Foot Prosthesis with a Bio-Inspired Controll Algorithm Successfully Reproduces Human Walking and Stair Ascent

Saturday Posters, Arranged by Lead Author (alphabetical)

	Lead Author	Title
	REGULAR MEMBERS	
S1	Tom Broderick	Acute Exercise Activates Pparα Expression and Carnitine Biosynthesis and Uptake in Mouse Kidney and Liver
S2	Taben Hale	Sex Differences in Cardiovascular Responses to Stress in Adult Rats Prenatally Exposed to Dexamethasone
S3	Jon Harrison	Body Position Effects On Hemolymph and Air Distribution in Insects
S4	Christos Katsanos	Effects of Increased Plasma Branched-Chain Amino Acids and Insulin on Muscle Protein Metabolism
S5	Thomas Pannabecker	Evidence for Paracellular Urea Transport in the Rat Inner Medullary Thin Limbs of Henle's Loops

	Lead Author	Title
	POST-DOCS	
S6	Cheng-Yu Chen	Structure Studies of Soluble Guanylate Cyclase by Paramagnetic NMR
S7	Christiane Danilo	The Role of Gut Microbiota in Cardiac Injury
S8	Megan Garlapow	Genetic and Genomic Response to Selection for Food Consumption in *Drosophila melanogaster*
S9	John Kanady	A Lymphedema-Inducing Mutation of Cx47, R259c, Alters Growth Pattern and Cx43 Processing in Rat Insulinoma Cells
S10	Robert LeMoyne	Preliminary computational emulation of a central pattern generator for gait
S11	Joshua Strom	University of Arizona Phenotyping Core: Advancing in Vivo Research
S12	Manal Zein-Hammoud	Myofascial Release-Induced Wound Healing in 3-Dimensional Bioengineered Tendons: Roles for Fibroblast Proliferation and Collagen Secretion

UNDERGRADS on next page

	Lead Author	Title
	UNDERGRADUATE STUDENTS	
S13	RussL Altabtabaee	Effects of Genistein Diet on Diabetic Jejunum Function and Histology in the Ob/Ob Mouse
S14	Nickolas De Leon	Does an Increase in Plasma Amino Acid Concentrations Stimulate Skeletal Muscle Protein Synthesis in Obese Humans?
S15	Shannon Gillespie	Is Variation in Vertebral Column Morphology Associated with Variation in Axial Musculature in Killifishes?
S16	Fernando Ivich	Localization and Distribution of TRPV4 on the Lens Epithelium
S17	Colleen Kerrigan	Temporal Expression of Cyclooxygense-2 Following Midline Fluid Percussion Injury in the Male Rat Brain
S18	Tara Mahmood	High Intensity Exercise Protects Skeletal Muscle from Complications of Doxorubicin Treatment
S19	Brittney McCormick	Differential Cardiovascular and Penile Responses to Angiotensin Ii and Bradykinin B1-Receptor Antagonism Treatment in Sprague-Dawley Rats
S20	Liam O'Neill	Evaluation of the Vasoprotective Effects of High-Intensity Exercise Prior to Antrhacycline Chemotherapy
S21	James Sargent	Age-Related Decline of Anoxia Tolerance in Adult *Drosophila Melanogaster*
S22	Nirmal Vijayavel	Doxorubicin Reduces Proinflammatory Mediator Expression in Brain and Pial Arteries from Ovariectomized Female Rats
S23	Julian Wagner	Hypermetric Tracheal Scaling as a Factor in Insect Gigantism

Friday's Abstracts

(Alphabetical, by first author--poster board # shown)

GRADUATE STUDENTS

F1

TGF-β/ALK1 Signaling Alters Organic Anion Transporting Polypeptide 1a4 (Oatp1a4) Expression at the Blood-Brain Barrier.

Wazir Abdullahi, Hrvoje Brzica, Kathryn Ibbotson, Patrick T. Ronaldson**.** *Department of Pharmacology, University of Arizona, Tucson, AZ, United States of America*

Introduction: Effective treatment of central nervous system (CNS) disease requires that drugs attain efficacious concentrations in the brain. One approach that can enable this therapeutic goal to be achieved is to target endogenous blood-brain barrier (BBB) transporters such as Oatp1a4. It is also critical to identify and characterize biological mechanisms that modulate BBB transport processes. The goal of the present study was to investigate, *in vivo*, the role of transforming growth factor beta (TGF-β) signaling via the ALK1 receptor on Oatp1a4 expression at the BBB.

Methods: Female Sprague-Dawley rats (200-250 g) were administered bone morphogenic protein-9 (BMP-9; 0-5 ug/kg), an established ALK1 agonist, via intraperitoneal injection. Time-matched control animals were injected with 0.9% saline instead of BMP-9. After 6 h exposure to BMP-9, animals were sacrificed and brain microvessels were isolated. Western blot analysis was used to determine protein expression of ALK1 and Oatp1a4.

Results: Western blot analysis demonstrated no change in expression of ALK1 in isolated brain microvessels from BMP-9 rats as compared to controls. No change in expression of Oatp1a4 was observed in animals exposed to 0.5 ug/kg BMP-9 for 6 h as compared to controls. In contrast, higher doses of BMP-9 (i.e., 2.5 ug/kg or 5.0 ug/kg) resulted in increased Oatp1a4 protein expression, suggesting a concentration-dependent effect.

Conclusions: Our current data implies that TGF-β signaling via ALK1 may play a role in altering Oatp1a4 protein expression at the BBB. Studies are currently underway to determine the intracellular signaling molecules (i.e., Smad proteins) involved in regulating this pathophysiological response as well as the functional implications of altered Oatp1a4 protein expression.

F2

THE EFFECT OF PRIOR SHORTENING ON RESIDUAL FORCE ENHANCEMENT AFTER STRETCH IN MOUSE MUSCLES.

RIFAT ARA ADITY, RAA, KIISA CARLA NISHIKAWA, KCN

The mechanism of muscle contraction was first explained by the sliding filament theory However, several muscle properties are poorly explained by this theory such as: 1) enhancement of force with stretch; and 2) depression of force with shortening. Recently, a new theory of muscle contraction, the "winding filament" hypothesis, has been suggested. This hypothesis explains how titin acts in conjunction with sliding filament - swinging cross-bridge theory. This theory resolves many unexplained muscle properties. Titin is a giant protein that spans the muscle half-sarcomere. It is composed of tandem immunoglobulin (Ig), N2A and PEVK segments. According to the winding filament hypothesis, the N2A region binds to actin upon calcium influx and the PEVK region winds on actin in active muscle. In the passively stretched condition, the PEVK region does not wind on actin because the N2A region does not bind. If activation of a passive elastic element is responsible for residual force enhancement, then shortening prior to stretch should reduce or eliminate the extra force upon stretch. Edman and others have performed experiments in which active muscles were shortened prior to stretch. However, they observed no reduction in residual force enhancement due to pre-shortening. They concluded that, if an elastic element is formed in muscle during activation, it is not slackened by shortening. Later studies showed that, as the delay between shortening and stretch increased, the effect of shortening on force enhancement decreased. The purpose of this study was to evaluate the effect of the delay between shortening and stretching in mouse muscles and to explore the idea that the winding filament hypothesis can explain the observed effects. Muscles were placed on the descending limb of the force-length relationship. The muscles were first shortened and then stretched at a fixed amplitude and speed (10% fiber length, and at 40% fiber length/s), either immediately following shortening, or 300, 400, 500, 600, 700 or 800 ms following shortening. As the interval between shortening and stretch increased, residual force enhancement increased. The observations are consistent with the existence of a structural elastic element in vertebrate skeletal muscle that develops upon muscle activation, as well as a time-dependent mechanism, such as cross-bridge cycling and titin winding, which takes up its slack following shortening.

F3

Mechanotransduction via Titin's N2B Element Contributes to Cardiac Remodeling.

Mathew Bull, Pooja Nair, Josh Strom, Michael Gotthardt and Henk Granzier

Pathological remodeling is responsible for the functional deficits characteristic of heart failure patients. Understanding mechanotransduction is limited, but holds potential to provide novel therapeutic targets to treat patients with heart failure, especially those with diastolic dysfunction and preserved ejection fraction (HFpEF). Titin is the largest known protein and is abundant in muscle. It is the main contributor of passive stiffness in the heart and functions as a molecular mechano-sensor for stress and strain in the myocyte. Titin is composed of four distinct regions, (N-terminal Z-line, I-band, A-band, and C-terminal M-line), and acts as a molecular spring that is responsible for the assembly and maintenance of ultrastructure in the sarcomere. The elastic N2B element found in titin's I-band region has been proposed as a mechano-sensor and signaling "hot spot" in the sarcomere. This study investigates the role of titin's cardiac specific N2B element as sensor for stress and strain induced remodeling in the heart. The previously published N2B knock out (KO) mouse was subjected to a variety of stressors including transverse aortic constriction (TAC), aorto-caval fistula (ACF), chronic swimming, voluntary running and isoproterenol injections. Through chronic pathologic stress, pressure overload (TAC) and chronic volume overload (ACF), we found that the N2B element is necessary for the response to volume overload but not pressure overload as determined by changes in cardiac remodeling. Furthermore, the response to exercise by chronic swimming was reduced in the N2B KO mouse. Finally, unlike the wild-type (WT) mouse, the N2B KO mouse did not respond to isoproterenol injections with hypertrophic remodeling. Ongoing work to elucidate the molecular pathways involving the N2B element and response to stress, is focused on its binding protein Four-and-a-half-LIM domains 2 (FHL2) and the mitogen activated protein kinase (MAPK) pathway. Taken together our data suggest that the N2B element contributes significantly to mechanotransduction in the heart.

F4

METABOLIC AND GENETIC IMPLICATIONS OF SURVIVAL IN ANOXIA

Jacob B. Campbell[1], Jon F. Harrison1, *Arizona State University*

Anoxia or severe hypoxia is a fundamental component of pathologies associated with heart disease, stroke and many other human pathologies; yet we still lack a fundamental understanding of how anoxia/severe hypoxia kills and the mechanisms responsible for the wide variation in anoxia tolerance across animals. *Drosophila* larvae feed on the yeasts of rotting fruits in a semiliquid environment, and as a consequence, the larvae regularly experience episodes of hypoxia/anoxia whereas adults live in air and are likely to experience hypoxia on rare occasions. Perhaps surprisingly, larvae are much less tolerant of anoxia than adults; nearly 100% of adults survive up to 4 hours of anoxia while less than 50% of third instar larvae survive anoxic bouts greater than 90 minutes. We used biochemical and physiological methods to assess stage-related variation in the ability to match ATP supply and demand, and in addition, we conducted a genome-wide association study to find and then verify candidate genes responsible for variation in anoxia survival within populations of larvae and adults. Anoxia induced strong decreases in glycogen levels in both larvae and adults; however, both stages also showed strong increases in free glucose indicating that carbohydrate depletion is likely not a cause of death. Both larvae and adults accumulated lactate, but larvae did so at a higher rate during the first hour of anoxic exposure which suggests that high locomotion of larvae during initial exposure to hypoxia requires high rates of anaerobic metabolism that may be functionally linked to mortality. Preliminary measures of ATP show that ATP declines to near zero at the first measured time points—2 hours for adults and 30 minutes for larvae. Survival of a 1 hour anoxia exposure was highly repeatable but varied greatly across 178 lines from the *Drosophila* Genetics Reference Panel ranging from 25-95%. Thirty-two SNPs and 23 genes were associated with the variation in survival across lines, all with P values less than 0.00001. Gene ontology enrichment analysis implicates gene classes involved in angiogenesis, cell proliferation, membrane and cytoskeletal remodeling, and fatty acid metabolism in the differential survival across lines. Several of the identified genes linked to survival across the DGRP lines have human orthologs that have been linked to multiple oxygen-mediated cancer pathways and Alzheimer's progression in humans. This research was supported by NSF IOS 1256745.

GRADUATE STUDENTS

F5

Drug Discovery: Lipidation of Connexin Mimetic Peptides Increases Efficacy in Gap Junction Inhibition

Cotter M.L., Boitano S., Vagner J., and Burt J.M., University of Arizona, Tucson, AZ

Peptides mimicking short, conserved sequences in the extracellular loops of connexins (Cxs) are commonly used as reversible inhibitors of gap junction channel (GJC)-mediated intercellular communication. These Cx-mimetic peptides also inhibit the diffusion of ions and small molecules across hemichannels (HCs), or unapposed hexameric Cx channels that have not yet docked with their HC counterparts on neighboring cells to form GJCs. The inhibitory actions of mimetic peptides derived from the extracellular loops of Cx43 have demonstrated therapeutic benefits, especially with regards to wound healing. However, such peptidomimetics are typically used at high concentrations (i.e. 100-200μM, IC50 ~20-30μM) to achieve block. Therefore, development of more potent inhibitors is critical. We hypothesized that lipidation of Cx mimetic peptides could improve their ability to localize to the plasma membrane and thus more effectively interfere with HC and GJC function. To quantitatively assess potency and efficacy of our novel lapidated Cx-mimetic peptides, the extent of gap junction-dependent propagation of mechanically-induced Ca2+ waves in confluent cultures of both Madin-Darby canine kidney epithelial cells expressing Cx43 (MDCK43) and rabbit tracheal
epithelial cells (RTECs) was monitored. Using this physiologically-relevant system, we conclude that lipidation greatly improves the inhibitory action of the peptide, increasing its potency by up to five orders of magnitude with an IC50 well into the picomolar range. Our results demonstrate that the lipidation approach is a powerful tool for increasing known Cx-mimetic inhibition of GJC communication and represents a paradigm for the development of HC, GJC and Cx-specific inhibitory drugs.

F6

IN THE SHORT TERM, POOR NUTRITION PROMOTES SIMPLE STEATOSIS WITHOUT INFLAMMATION IN ADOLESCENT RATS

Crawford M, Liss T, Calhoun M, Sweazea KL.
Arizona State University, Tempe, AZ

The development of hepatic steatosis in adults has been linked to high caloric intake. However, less is known about the physiological consequences of this disease during adolescence. The present study examined the association of high caloric intake and hepatic steatosis in adolescent rats. Six-week old male Sprague-Dawley rats were fed one of the following diets: standard rodent chow (18.9% protein, 57.33% carbohydrates), high-sucrose (20% protein, 70% carbohydrates (34.5% sucrose), 10% fat) or high-fat (20% protein, 20% carbohydrates (6.8% sucrose), 60% fat) for 6 weeks. Following the 6 week diet, animals were euthanized (sodium pentobarbital; 200 mg/kg, i.p.) and livers extracted for analyses. An increase in Oil Red O stained areas of liver sections provided evidence for the development of steatosis in the HF fed animals, but not the HS fed animals, that was confirmed by increased triglyceride concentrations in the liver as compared to animals fed the chow or HS diets (20.73 ± 2.09, 9.75 ± 0.52, and 10.76 ± 0.74 mg triglycerides/g tissue, respectively; $p < 0.001$). Despite the observed steatosis, western blot analyses showed no significant differences between groups in proteins associated with insulin signaling (PI3K), gluconeogenesis (PEPCK-C), immune response (XBP1), inflammation or oxidative stress (TLR-4, iNOS). The short feeding protocol used in the current study may explain the lack of measurable alterations in protein expression as others typically examine the effects of high caloric diets for 8-12 weeks before measuring changes. Together these findings suggest that short term high fat intake promotes simple steatosis in the absence of changes in insulin signaling or inflammation.

F7

CAPN10 and ADCY5 SNPs are associated with obesity-related phenotypes and DNA methylation in human skeletal muscle

Day SE, Campbell LE, Coletta RL, Kim JY, Benjamin TR, Roust LR, DeFilippis EA, Dinu V, Shaibi GQ, MandarinoLJ, Coletta DK
Arizona State University, Tempe, AZ

Obesity associated insulin resistance is a major risk factor for the development of type 2 diabetes (T2D) and cardiovascular diseases. The role of DNA methylation in obesity is not well understood. Additionally, single nucleotide polymorphisms (SNPs) at CpG sites can alter the methylation status of the genome, which could alter gene expression. Vastus lateralis muscle biopsies were taken during a euglycemic-hyperinsulinemic clamp, and reduced representation bisulfite sequencing was performed on the DNA from obese (n=10; BMI=32.9±0.7 kg/m2) and lean (n=12; BMI=23.4±0.7 kg/m2) subjects. There were 99,748 differentially methylated cytosines (DMCs; P<0.05) captured, and 8,399 were associated with a SNP. Furthermore, we set out to identify CpG-SNPs with a methylation difference >20% and minor allele frequency >5% that were associated with previously known obesity and T2D genes. DNA methylation was significantly different for SNP rs3749166 in calpain 10 (CAPN10; A/A 0±0, A/G 0.37±0.2, G/G 0.96±0.05 methylation ratio; P<0.001) and SNP rs4678009 in adenylate cyclase 5 (ADCY5; C/C 0.6±0.1, T/T 0.2±0.1 methylation ratio; P<0.001). The A allele for CAPN10 was associated with increased blood pressure (A/A 125/78, A/G 123/76, G/G 114/69 mm/Hg; P<0.05) and trended towards an association with BMI (A/A 30.2±5, A/G 28.3±5, G/G 23.0±3 kg/m2; P=0.06). The C allele for ADCY5 was associated with increased BMI (C/C 29.2±5.5, T/T 24.4±3.5; P≤0.05) and decreased insulin sensitivity (clamp Rd; C/C 5.4±2.5, T/T 7.5±1.6, P≤0.05). The present study provides evidence that CpG-SNPs in CAPN10 and ADCY5 alters DNA methylation, which may contribute to obesity and its related phenotypes.

F8

HIGH INTENSITY EXERCISE PRESERVES MYOCELLULAR SIZE THROUGHOUT DOXORUBICIN TREATMENT

AC D'Lugos, T Mahmood C Cosgrave, WL Dedmon, BD Astill, S Patel, M Katsma, RJ Gonzales, TM Hale, CC Carroll, SS Angadi, and JM Dickinson
Arizona State University, Phoenix, AZ; Midwestern University, Glendale, AZ; University of Arizona, Phoenix, AZ

Anthracyclines are mainstay chemotherapeutic agents proven effective to reduce disease recurrence and mortality of breast cancer patients. However, these drugs also have devastating side effects that include skeletal muscle wasting. The purpose of this study was to assess the impact of bi-weekly doxorubicin (DOX) administration on body weight and skeletal muscle fiber size, and secondarily, to assess the ability of high-intensity interval exercise training before and during DOX treatments to attenuate reductions in body weight and fiber size. We hypothesized that DOX treatment would reduce body weight and skeletal muscle size, and that exercise would attenuate this response. Eight-week old ovariectomized female Sprague-Dawley rats were randomized to one of four treatments: Exercise+DOX (Ex-DOX); Ex+Vehicle (Ex-veh), Sedentary+DOX (Sed-DOX); and Sed+veh (Sed-veh). DOX (4mg/kg) or vehicle (saline) intraperitoneal injections were performed bi-weekly for a total of 3 injections (cumulative dose 12mg/kg). Ex animals underwent exercise 5d/week starting one week prior to the first injection and continued throughout study duration. Animals were euthanized ~5d following the last injection, during which the soleus muscle was dissected and prepped for immunohistological analysis. Relative to Sed-Veh, body weight was similarly reduced in Sed-DOX and Ex-DOX ($p<0.05$ vs. Sed-Veh and Ex-Veh). Cross-sectional areas (CSA) of myosin heavy chain (MHC) I and MHCIIa fibers of Sed-DOX were 30% smaller than Sed-Veh ($p<0.05$), whereas CSA of MHCI and MHCIIa were only reduced by 12% in Ex-DOX ($p<0.05$ vs. Sed-Veh). Further, fiber CSAs were larger in Ex-DOX vs. Sed-DOX indicating the preservation of muscle fiber size. These preliminary data suggest that DOX administration may reduce MHCI and MHCIIa fiber CSA, and that independent of changes in animal weight, intense exercise training may provide a therapeutic strategy to preserve skeletal muscle size during chemotherapy treatment.

F9

DOPAMINE MODULATES THE PRE-SYNAPTIC UNEVOKED RELEASE OF GLYCINE IN THE INNER RETINA

Flood MD, Mazade RE, Eggers ED

In order to maintain a proper signaling response to light, the retina must constantly tune its sensitivity to ambient luminance conditions, a process termed "light adaptation." A large body of evidence suggests that dopamine is the major neuromodulator responsible for light adaptation in the retina; however, the mechanisms through which dopamine causes these changes are largely unknown. In the retina, photoreceptors transduce light stimuli into excitatory signals that are sent to ganglion cells (GCs) via bipolar cells (BCs). This excitatory signaling pathway is modulated by inhibitory inputs from amacrine cells (ACs), through the release of the inhibitory neurotransmitters glycine and GABA onto BCs.Additionally, BCs, ACs and GCs all express dopamine type 1 receptors (D1Rs), which act through a second messenger system to produce intracellular changes upon binding of dopamine. Previous data collected in our lab showed that light adaptation decreased the frequency and amplitude of spontaneous inhibitory currents, the equivalent of signal "noise", in OFF BCs, which respond to the offset of light. It was also discovered that the majority of these currents were mediated by glycine instead of GABA.We hypothesized that treatment of retinas with the D1R agonist SKF would mimic the effect of light adaptation on this inhibitory noise, through modulating the release of neurotransmitter from ACs and/or the receptor sensitivity in OFF BCs. Using whole cell patch clamp and GABA receptor antagonists to isolate glycinergic activity, we measured the spontaneous inhibitory post-synaptic currents (sIPSCs) from OFF BCs in dark-adapted retinas before and after SKF. To differentiate between pre- and post-synaptic changes we then performed the same experiments after blocking voltage-gated channels with cadmium and tetrodotoxin, in order to isolate spontaneous miniature inhibitory post-synaptic currents (mIPSCs) that come from the spontaneous release of one vesicle of neurotransmitter. We found that SKF caused a decline in both amplitude and frequency of sIPSCs, similar to that seen in light-adapted retinas. We found no difference in peak amplitude, frequency, or decay constant of the mIPSCs upon SKF treatment. Our results suggest that dopamine is sufficient to mimic the effects of light adaptation on spontaneous glycinergic inhibition to OFF BCs, and that it does so by reducing release of neurotransmitter from ACs.

F10

Evaluation of the effects of mild aerobic exercise on aortic contraction in a mouse model of Marfan syndrome

[1,2]Christine P. Gibson, [1]Ramona Alex, [2]Tom Broderick, [1]Kim Cooper, [2]Johana Vallejo-Elias, and [1]Mitra Esfandiarei, [1]Department of Biomedical, Sciences College of Health Sciences, [2]Department of Physiology, Arizona College of Osteopathic Medicine, Midwestern University, Glendale, AZ

Aortic aneurysm is the leading cause of death in Marfan syndrome (MFS), a connective tissue disorder caused by mutations in fibrillin-1 gene. MFS aneurysm is characterized by weakening of the aortic wall due to elastin fibers fragmentation. The above-average height and distinct physical features make young adults with MFS desirable candidates for competitive sports; but little is known about the exercise limit at which they will be at risk for aortic rupture. On the other hand, voluntary and forced cardiovascular exercise has been shown to have a protective effect on the aortic wall. In this study, we propose that a voluntary (wheel cage) or a forced (treadmill) aerobic exercise routine will improve the function (vasoconstriction and vasodilation) of the aorta in a mouse model of MFS. Four-week old control and MFS mice were subjected to voluntary wheel exercise, forced treadmill exercise, or sedentary life-style for five months. Thoracic aortic rings were isolated at the age of 24 weeks, and subjected to functional studies using wire myography. We observed that compared to age-matched controls, MFS mice covered significantly less distance (37% less) per day during the voluntary group study period. In addition, compared to non-exercise MFS mice, aortic vessel contractility (in response to vasoconstrictor drug phenylephrine) demonstrated no improvement in both voluntary and forced exercise MFS mice. Dilation of the aortic vessel (in response to vasodilator agent acetylcholine) was significantly improved in both voluntary and forced exercise MFS mice. These findings provide new insights into the potential protective effects of mild exercise routine in Marfan patients in the absence of pharmacological interventions, especially in young adults affected by cardiovascular complications and aortic aneurysm. This work was funded by Midwestern University Research Fund and the Canadian Institutes of Health Research.

F11

Mild aerobic exercise improves aortic wall integrity and elasticity in a mouse model of Marfan syndrome

[1,2]Christine P. Gibson, [1]Ramona Alex, [2]Tom Broderick, [1]Kim Cooper, [2]Johana Vallejo-Elias, and [1]Mitra Esfandiarei, [1]Department of Biomedical, Sciences College of Health Sciences, [2]Department of Physiology, Arizona College of Osteopathic Medicine, Midwestern University, Glendale, AZ

Marfan syndrome (MFS) is a connective tissue disorder due to mutations in fibrilin-1 gene. Aortic aneurysm is the most life-threatening complication in MFS patients. MFS associated aneurysm is characterized by weakening of the aortic wall due to elastin fibers fragmentation and disorganization. Previous studies have shown that cardiovascular exercise has a protective effect on the aortic wall. However, little is known about the exercise limit at which Marfan patients will be at risk for aortic rupture. In this study, we propose that a voluntary (wheel cage) or a forced (treadmill) aerobic exercise routine will improve the structure, including blood vessel wall integrity, elasticity, and elastin density, of the aorta in a mouse model of MFS. Four-week old control and MFS mice were subjected to voluntary wheel exercise, forced treadmill exercise, or sedentary life-style for five months. Thoracic aortic rings were isolated at the age of 24 weeks, and subjected to structural studies using histology and wire myography (for elasticity studies). We observed that compared to age-matched controls, MFS mice covered significantly less distance per month during the voluntary wheel cage group study period. In addition, compared to non-exercise MFS mice, aortic wall structure (elastin fibers organization, elastin density, and aortic wall integrity) were significantly improved in both voluntary and forced exercise MFS mice. These findings provide new insights into the potential protective effects of mild exercise routine in Marfan patients in the absence of pharmacological interventions, especially in young adults affected by cardiovascular complications and aortic aneurysm. This work was funded by Midwestern University Research Fund and the Canadian Institutes of Health Research.

F12

Caveolae as Potential Regulators of TGF-β and AT_1R Signaling in Aortic Smooth Muscle Cells.

[1] Harmon J., [2]Leung, L., [1]Esfandiarei, M. and [2]Vallejo J., [1]Biomedical Sciences and [2]Physiology Department, Midwestern University, Glendale AZ

Aortic aneurysm and progression to rupture is primarily the consequence of deregulation of transforming growth factor-β (TGF-β) and angiotensin II type 1 receptor (AT_1R) signaling cascades. There are many cell types contributing to aortic structure with smooth muscle cells being the dominant phenotype. The pathological state of aortic aneurysm can be greatly attributed to deregulation of the Smad2 and MAPK signaling cascades through activation of TGF-β and AT_1R receptors. Although TGF-β and AT_1R signaling cascades contribute to aortic aneurysm, the relative contribution of these pathways is currently unknown, particularly in smooth muscle. Interestingly, both signaling pathways have been found to be regulated by a special type of lipid raft domain known as caveolae. Caveolae has been reported to inhibit TGF-β receptor (TGF-βR) signaling while at the same time facilitate AT_1R signaling in fibroblasts and endothelial cells. Animal models of aortic aneurysm are both costly and lack the tightly controlled system required to elucidate the specific contribution of these complicated signaling pathways within diverse cell types in the aorta (e.g. endothelium, smooth muscle, fibroblasts). Because of this we have first chosen to establish a cell culture model of rat aortic smooth muscle cells (A7r5). In this model we have manipulated TGF-β receptor signaling by stimulation with TGF-β1 and AT1R signaling by stimulation with Ang-II. Pathway interaction and convergence was further established by activating both pathways simultaneously. To investigate the regulatory role of caveolae in TGF-β and AT_1R signaling pathways, experiments were carried out with and without disruption of caveolae lipid raft domains by treatment with methyl-β-cyclodextrin. After treatments, whole cell lysates were subjected to Western blot analysis of TGF-βR, Smad2, pSmad2/3, AT_1R, ERK1/2, pERK1/2, JNK, pJNK, Cav-1, and GAPDH proteins. Based upon the results of this study in our model of aortic smooth muscle cells, TGF-β signaling appears to play a much greater role in activation of Smad2 and MAPK signaling cascades than does Ang-II. Caveolae disruption did not appear to alter the ability of TGF-β to activate Smad2 and MAPK signaling cascades. The expression of the caveolae protein Cav-1 did not appear to change with treatment of TGF-β and Ang-II as had been previously reported in fibroblast and endothelial cells.

F13

Experience-dependent changes in vocal production in male rats.

Hernandez C, Sabin M, Riede T; Midwestern University

Complexity of a behavior repertoire might be simplified by the presence and combination of fixed patterns (="modules"). By activating modules and combining those modules in a context-specific way, the nervous system may effectively reduce the degrees of freedom associated with producing context-specific complex behavior. Vocal communication is a complex behavior, and data are accumulating in songbirds and mammals that it is generated from discrete smaller units or modules. We have proposed that parts of rat ultrasonic vocalization (USV) which play an essential role in their social organization, show features of a modular behavior. For their spectrographically and functionally diverse repertoire of 50 kHz calls, rats appear to rely on a small set of modules which are linearly (re-) combined. It was not clear if modularized recruitment of stereotyped motor patterns applies to the entire ultrasonic vocal repertoire. Here we show that rats combine also 22 kHz calls with 50 kHz calls into a single utterance, and that the distinct usage of 22 kHz and 50 kHz calls occurs subsequent to experience. The results suggest that the entire ultrasonic vocal repertoire of rats consists of modules, and that the vocal repertoire of an adult rat is not entirely innate.

F14

AN EVALUATION OF ECCENTRIC CONTRACTION FUNCTION DURING A STRETCH SHORTENING CYCLE FOR MUSCLES IN MICE

Hessel AL, Miyano CA, Felix I, Elbert AL, Olson KE, Nishikawa KC.

During animal movement, muscle length oscillations are common. We used a stretch-shortening cycle (SSC) protocol that stimulated muscles over the first third of lengthening to determine eccentric contraction properties during cyclical length changes. Mouse extensor digitorum longus (EDL, fast twitch) and soleus (slow twitch) muscles were used in the experiments. Additionally, due to the attenuation of eccentric contraction properties in *mdm* mice, these muscles were evaluated under the SSC protocol and results compared to wild-type muscles. We calculated the rate of force development (RFD) during eccentric contractions and total work. The results indicate that the RFD is larger in the EDL than the soleus, while both have larger RFDs than isometric contractions. Both EDL and soleus display large negative work, showing their absorptive properties during eccentric contractions. It is apparent that the EDL and soleus differ in muscle deactivation rates; the soleus maintains force well after stimulation ends while the EDL drops in force immediately after deactivation. We suggest that this is caused by the differences in calcium uptake rates. These results suggest that the soleus functions as a spring, while the EDL functions as a shock absorber. *Mdm* muscles showed reduced RFD and negative work compared to wild-type muscles, suggesting that a key component of the eccentric contraction mechanism is lost by the *mdm* mutation. The *mdm* mutation involves a deletion in part of the N2A region of titin, which could be involved in titin activation for eccentric function - a prediction of the winding filament hypothesis. Taken together, the SSC approach used here appears to be a good strategy to study and compare mechanics of different muscles with varying fiber types and functions.

F15

PLASMA FREE FATTY ACID AND AMINO ACID RESPONSES TO GLUCOSE-INDUCED INSULINEMIA IN INSULIN-RESISTANT SUBJECTS

Hoffman N., Tran L., Carroll C., Eldon. E, Patel. S., Katsanos CS.
School of Life Sciences and Center for Metabolic and Vascular Biology, Arizona State University and Mayo Clinic in Arizona, Scottsdale, AZ and Department of Physiology, Midwestern University, Glendale, AZ

Insulin-resistant individuals have impaired insulin-mediated plasma glucose metabolism, but the effects of the insulin on plasma free fatty acid (FFA) and amino acid metabolism are less known. Using the Matsuda Insulin Sensitivity Index (ISI), we identified a group of insulin-sensitive (IS; gender, 3M/3F; age, 42±3 years; BMI, 23±1; ISI, 10.9±0.8; mean±SE) and insulin-resistant (IS, 5M/4F; age, 35±3 years; BMI, 35±1; 2.8±0.4) subjects (P<0.05 between groups for BMI and ISI). Insulinemia was induced by the ingestion of bolus of glucose (75g). Plasma insulin concentration (uIU/ml) increased from basal (IS, 3.5±0.5; IR, 13.5±1.9*; P*<0.001) more in the IR subjects by 30 min and remained elevated in the IR subjects until end of the study at 120 min (IS, 20±4 ; IR, 92±15; P<0.001). Fasting plasma total FFA concentrations (mmol/l) tended to be higher in the IR group (0.42±0.07 vs 0.62±0.06*; P*=0.07) and decreased throughout the study in both groups, remaining lower in the IS than the IR at 30, 60, 90, and 120 mins (P<0.05). Fasting concentration of plasma total amino acids (TAA; umol/l) was not different between groups (IS, 2618±148; IR, 2588±178*; P*>0.05) and decreased over the course of the 120 min in both groups, and they were lower in the IS than the IR at 60 min (P<0.05). The decrease in the TAA was due to a decrease in essential amino acid (EAA). Fasting EAA were not different between groups (IS, 913±54; IR, 1011±74*; P*>0.05), but were lower in the IS group at 30 and 60 min (P<0.05) mins. Non-EAA were not different between groups at any of the time points (P>0.05) We conclude that during glucose-induced insulinemia IR individual have lower suppression of plasma FFA and amino acid concentrations by insulin. Although this effect is documented at the total plasma FFA level, it is only evident in selected plasma amino acid concentrations (i.e., EAA).

F16

GAP JUNCTION CHANNEL CONDUCTIVITY DOES NOT PREDICT INSULINOMA CELL PROLIFERATIVE PHENOTYPES INDUCED BY CONNEXIN 37 PHOSPHO-ISOFORMS

NL Jacobsen, TK Pontifex, and JM Burt
Physiological Sciences GIDP, Department of Physiology, University of Arizona, Tucson, AZ

Expression of connexin 37 (Cx37), but not Cx40 or Cx43, potently suppresses the growth of highly proliferative rat insulinoma (Rin) cells. Expression of Cx37 mutants that are unable to form functional channels or do not include the carboxyl-terminal (CT) regulatory domain do not suppress Rin cell proliferation, like Cx37-WT. Since proliferation is mediated by growth factor-activated kinases, we hypothesized that the CT regulates growth in a site-specific manner. Expression of Cx37 with aspartate substitutions (to mimic phosphorylation) at 7 high probability phosphorylation sites in the CT-regulatory domain (serines 275, 285, 302, 319, 321, 325, 328; Cx37-S_7D_7) induced caspase-dependent cell death after 4 days of induced expression. In contrast, aspartate substitution at only serines 275, 319, and 328 (putative MAPK, GSK-3, and PKC, respectively; Cx37-S_3D_3) alleviated Cx37-mediated growth suppression, as expression of Cx37-S_3D_3 had no effect on Rin cell proliferation. To determine if mimicking phosphorylation within the CT modulates channel function in a manner predictive of these different phenotypes (controlled growth (Cx37-WT), cell death (Cx37-S_7D_7) and proliferation (Cx37-S_3D_3), we examined channel conductive properties. Cx37-WT and Cx37-S_7D_7 form functional gap junction channels that predominantly reside in a subconductance state (~80pS), but can transition to a variety of open states including the fully open channel (~370pS). Cx37-S_3D_3 channels frequently transitioned between a ~60pS substate and the fully open channel (~400pS), spending more time in the fully open conformation than either Cx37-WT or Cx37-S_7D_7. These data suggest that phosphorylated forms of the channel that support frequent activity of the fully open channel may be indicative of a growth permissive state. However, given the similarity between frequency of channel conductance states of Cx37-WT and Cx37-S_7D_7, it appears that conductivity of the channel alone is not predictive of the growth suppression or cell death that Cx37 may induce. Instead, these phenotypes may be determined by differences in the selective permeability of the channels, the binding partners of Cx37, or yet to be identified phosphorylation sites.

F17

Integrin β4 mRNA splicing patterns are influenced by SNPs

Kelly, GT, Mascarenhas, JB, Cress, AE, Garcia, JGN, Wang, T
College of Medicine, The University of Arizona, Tucson, AZ

Integrin β4 (*ITGB4*) is an important transmembrane receptor protein involved in cellular signaling and cell-matrix communication. ITGβ4E is the smallest splicing variant of *ITGB4* that misses a major portion of its intracellular domain, leading to some defects in signaling capacities. The genetic impact on *ITGB4* splicing to ITGβ4E variant is largely unknown.

In order to study the influence of single-nucleotide polymorphisms (SNP) on *ITGB4* splicing, minigenes were constructed containing exon 21, intron 21-22, and exon 22 of the *ITGB4* gene with either complete wild type (WT) sequence, or with point mutations to reflect chosen SNPs.

The sequence of *ITGB4* gene shows that four isoforms (A, B, C, and D) of Integrin β4 are created by complete removal of intron 21-22, but inclusion of 37 bps of the intron would produce the E isoform. Computational screening using a Bayesian splice center analysis predicted two SNPs in exon 21 and five in intron 21-22 that might affect splicing at the 5' end of intron 21-22. Rs372551314 in intron 21 was predicted to strengthen the normal splice site recognition by splicing machinery, and rs54619665 in intron 21-22 was predicted to decrease recognition. Following RT-PCR analysis, WT minigene created two bands, with the more prominent band at 95 bp representing long ITGβ4s (A, B, C or D) and a much weaker band at 132 bp, representing ITGβ4E. Rs372551314 containing minigene created similar patterns, with higher intensity in the 95 bp band (long ITGβ4s). Rs54619665 minigene resulted in complete loss of the 95 bp band and high intensity in the 132 bp band. These minigene data validated computational predictions.

In conclusion, utilization of computational prediction and minigene validation methods fully confirmed the genetic impact of SNP on *ITGB4* splicing in production of ITGβ4E, leading to a novel mechanistic explanation of ITGβ4E expression regulation.

F18

THE ENZYME NAGARSE IMPROVES PURITY AND FUNCTIONAL COUPLING OF SKELETAL MUSCLE SUBSARCOLEMMAL MITOCHONDRIA PREPARATIONS

Kras K.[1,2], Willis W.[1,2], Barker N.[2], Czyzyk T.[2], Langlais P.[2], Katsanos C.[1,2]
Arizona State University and Mayo Clinic in Arizona, School of Life Sciences and Nutrient Metabolism Lab, Scottsdale, AZ 85259

Skeletal muscle mitochondria (MITO) are arranged as a reticulum. Viewing the reticulum as a compartmentalization of "subsarcolemmal" (SS) and "intermyofibrillar" (IMF) regions, provides insight into the functional characteristic of MITO within the reticulum. A majority of published studies have reported lower (sometimes 2-fold) mitochondrial function and citrate synthase specific activities in SS compared to IMF mitochondria. The following hypothesis was tested; non-mitochondrial protein contamination accounts for the majority of lower activities of isolated SS mitochondria. Mouse gastrocnemius muscles (n = 6) were suspended in isolation medium, minced, and homogenized according to the procedures typically used to isolate SS mitochondria. After the first slow speed (800 x g) centrifugation, the supernatant was divided equally into two separate samples: one sample was exposed to nagarse (MITO+), while the other was not (MITO-). Three additional high-speed centrifugations were used to pellet and wash these two MITO preparations. Nagarse treatment altered the composition and function of the final mitochondrial suspension: MITO+ had reduced total protein content relative to MITO- (2.12±0.23 vs 2.80±0.37 $mg^{-1}.ml^{-1}$; $P<0.05$). MITO+, relative to MITO-, showed higher respiration rates (nmol O_2 $min^{-1}.mg^{-1}$) under state 4 conditions (31.0±3.5 vs 22.5±2.5; $P<0.05$), as well as higher maximal state 3 rates (138.7±16.8 vs 80.7±10.7; $P<0.05$). Therefore, the respiratory control ratio (state 3/state 4) was higher in MITO+ (4.5±0.2 vs 3.7±0.4; $P<0.05$). Mass spectrometry analysis showed MITO+ had a higher ratio of the averaged ion abundance associated with mitochondrial proteins versus non-mitochondrial proteins, compared to MITO- (7.2±1.2 vs 4.0±0.2; $P<0.05$). We conclude nagarse treatment of SS mitochondrial fraction proteolyzes non-mitochondrial and uncoupled mitochondrial proteins, improving indices of overall mitochondrial function and mitochondrial-specific activities, which more closely approach those previously determined in IMF MITO.

F19

ANGIOTENSIN II MODULATES SEX STEROID METABOLIZING ENZYME AND RECEPTOR EXPRESSION IN CARDIAC FIBROBLASTS FROM MALE AND FEMALE RATS

L Madhavpeddi, TM Hale, RJ Gonzales. Basic Medical Sciences Department, University of Arizona College of Medicine, Phoenix, AZ.

Pathological cardiac remodeling involving fibrosis is a major underlying feature of progressive heart disease leading to heart failure. Gonadal sex steroids have been shown to attenuate angiotensin II (AngII)-induced cardiac fibrosis and fibroblast activation. Given that AngII has been shown to influence androgen and estrogen receptor expression in non-cardiac tissues, in the present study we investigated the impact of AngII on sex steroid receptor and enzyme expression in primary rat cardiac fibroblasts. Cardiac fibroblasts were isolated from adult male and female rats and treated at passage 1 in 2% charcoal-stripped FBS for 24 hours with AngII or vehicle (Veh). Gene expression of aromatase, 5α-reductase, androgen receptor (AR), and estrogen receptors (ERα, ERβ) were determined by qRT-PCR. Cardiac fibroblasts express ERα, ERβ, and AR, as well as the metabolizing enzymes 5α-reductase and aromatase; however, levels of expression were not influenced by sex. AngII significantly and equivalently reduced mRNA expression levels of ERβ, ERα, AR, and 5α-reductase in both male and female cardiac fibroblasts. Aromatase was expressed at low levels in male and female fibroblasts and was not altered by AngII. In separate studies the impact of testosterone, a potential substrate for local 17β-estradiol production via aromatase, was assessed to indirectly determine if AngII alters local aromatase activity. Fibroblasts isolated from male rats were treated with testosterone for the final 6 hours of AngII incubation. However, the addition of testosterone did not alter AngII effects on sex steroid receptor or enzyme gene expression, nor levels of 17β-estradiol in the culture media. These findings demonstrate that AngII downregulates the local sex steroid receptor expression and at least one enzyme involved in gonadal sex steroid metabolism. Given the previously-described protective effects of testosterone and 17β-estradiol, the downregulation of androgen and estrogen receptors in cardiac fibroblasts may contribute to the cardiac fibrosis induced by AngII in both males and females.

Funding: AHA 13BGIA14720053

F20

CONTRIBUTES TO REDUCED JEJUNUM CHLORIDE SECRETION

Masood, F., Catmull, S., Leung, L., Arthur, K., and L. Al-Nakkash. Department of Physiology, AZCOM, Midwestern University, 19555 N. 59th Avenue, Glendale, AZ. 85308.

Obesity and diabetes are often associated with disturbances in intestinal function, i.e. slowed gastrointestinal transit. The objective of this study was to characterize jejunal function in a clinically relevant model of diabetes and obesity: the leptin-deficient *ob/ob* mouse. We measured transepithelial short circuit current (I_{sc}), across freshly isolated segments of jejunum from 10-11-week old *ob/ob* and lean C57Bl/6J male mice. Separate segments of jejunum were frozen for western blot determination of key proteins involved in secretory transport. Basal I_{sc} was significantly decreased in *ob/ob* mice (54.0 ± 6.9 μA/cm^2, n = 11, $P < 0.05$) compared to lean mice (84.5 ± 12.2 μA/cm^2, n = 10). Inhibition with clotrimazole and ouabain (both 100 μM, basolateral) was significantly reduced in *ob/ob* mice compared to lean mice ($P <$ 0.05). Expression of total CFTR (normalized to GAPDH) was significantly decreased 2-fold ($P < 0.05$) in *ob/ob* mice compared to lean mice. Feeding a sub-group of *ob/ob* male mice a 600 mg genistein/kg diet for 4-weeks, resulted in a significant 2-fold increase in basal I_{sc} (108.9 ± 9.4 μA/cm^2, n = 7, $P < 0.05$). Our data suggests that the reduced basal jejunal I_{sc} in *ob/ob* mice is a consequence of reduced CFTR expression, decreased activity of the basolateral K_{Ca} channel and Na^+/K^+-ATPase, each of which likely contributes towards this phenotype in jejunum of the *ob/ob* mouse. Genistein diet appears to have beneficial effects on basal I_{sc}. Understanding these intestinal dysfunctions in the *ob/ob* jejunum, may allow for the development of novel drug targets to treat obesity and diabetes, and may also be of benefit in CF-related diabetes. Supported by: Soy Health Research Program, Diabetes Action Research and Education Foundation, and MWU intramural funds.

F21

ARE THERE PERFORMANCE TRADEOFFS IN THE ABILITY TO PERFORM THE AQUATIC C-START AND TERRESTRIAL TAIL-FLIP JUMP? Minicozzi M. Finden A. Gibb A. C. Northern Arizona University, Flagstaff AZ

The killifishes (Cyprinodontiformes) usually respond to a negative aquatic stimulus by performing an aquatic escape, or C-start, but some killifish species voluntarily jump out of the water and onto land when threatened. Once on land, these fish typically perform a tail-flip jump to return to the water. During the tail-flip jump, a fish raises its head from the substrate and bends towards its tail, forming a "C", then straightens its body while pushing off of the substrate with the caudal peduncle to launch into ballistic flight. This behavior shares key similarities with the aquatic escape response, including large amplitude lateral bending, followed by axial straightening. However, the tail flip jump must be performed against the forces of gravity and over a longer time interval, relative to the aquatic escape response. Because the mechanical demands on the musculoskeletal system are different on water vs. land, we hypothesized that there would be functional tradeoffs between the C-start and the tail-flip jump. We predicted fishes that perform better (longer) terrestrial jumps would perform worse (slower) aquatic C-starts. To test this prediction, we examined three species of killifish: *Gambusia affinis, Poecilia mexicana,* and *Jordanella floridae.* We filmed individuals (n=10) of all three species in high speed performing the C-start in water (800 fps) and tail-flip jump on land (600 fps). In contrast with our original prediction, we found no functional tradeoff between C-start and tail-flip jumping performance. Fishes that performed faster C-starts also tended to perform longer tail-flip jumps. This suggests that the selection pressures that underlie the evolution of both of behaviors may generate a body shape that is capable of producing effective movements in both environments, despite the drastic physical differences between the aquatic and terrestrial realms.

F22

STRETCH SHORTENING CYCLE PROTOCOLS DEMONSTRATE THE AGE ASSOCIATED DIFFERENCE IN ECCENTRIC PROPERTIES OF EDL AND SOLEUS MUSCLES

Miyano C, Hessel AL and Nishikawa KC, Northern Arizona University, Flagstaff, Arizona

The purpose of this study was to evaluate eccentric muscle forces during oscillating muscle length changes. This study used a stretch-shortening cycle (SSC) protocol that stimulated muscles over the first third of lengthening to determine eccentric contraction properties during length oscillations in mice that range in age from 30 - 400 days. During animal movement, cyclical changes in muscle length are common. However, age-associated muscle mechanics are not well understood. Mouse extensor digitorum longus (EDL, fast twitch) and soleus (slow twitch) muscles were used in the experiments. We calculated the rate of force development (RFD) and total work during eccentric contractions. A passive SSC was also conducted to measure passive properties, because an age-associated increase in muscle stiffness was expected. The results indicate that the RFD and total negative work increased with increasing age. These results appear to indicate that active muscle stiffness increased with age. The contribution of passive muscle components remained consistent or increased only slightly with age. These results suggest that the increase in muscle stiffness with age is associated with components of active muscle. These could include age-associated changes in cross bridge cycling or an increase in stiffness of the titin filament. Titin has been shown to contribute to passive and active stiffness in eccentrically contracting muscles. Because titin stiffness is modified by a variety of pathways, we believe future work should focus on identifying age-associated changes in titin stiffness.

F23

FOXP3+ REGULATORY T CELL DEPLETION ELIMINATES ANG IIINDUCED HYPERTENSION RESISTANCE IN FEMALE MICE. Pollow DP, Romero-Aleshire MJ, Uhrlaub J, Nikolich-Zugich J, Brooks HL. University of Arizona, Tucson, Arizona.

Compared to males, premenopausal females are resistant to the development of Ang II hypertension. In males, Ang II induces hypertension, in part, through mechanisms requiring T effector lymphocytes. Recently, our lab has demonstrated that females can prevent the T lymphocytedependent increase in blood pressure (SBP and MAP) and expression of proinflammatory cytokines in the kidney in response to Ang II infusion. Because Foxp3+ T regulatory cells suppress the pro-inflammatory and hypertensive actions of T effector cells, we sought to determine whether Foxp3+ T regulatory cells contribute to this resistance in females. Premenopausal (8 week old) 129SVE female mice were infused with Ang II (800ng/kg/min, 14d) and received 4 doses of the anti-CD25 antibody PC-61 to transiently deplete Foxp3+ T regulatory cells (every 84 hours beginning 12 hours prior to Ang II infusion, 250µg/dose, i.p., vehicle control). Blood pressure was measured before and after Ang II infusion via non-invasive tail cuff. Ang II induced a significant increase in systolic blood pressure in Foxp3+-depleted mice, while resistance was retained in vehicle-treated mice (Con Δ5 + 5mmHg, Ang II Δ10 + 7mmHg, PC-61 Δ28 + 9*mmHg, *p<0.05 vs Con). Flow cytometric analysis demonstrated that PC-61-treatment significantly
reduced the number of Foxp3+ splenic T cells compared to control (Con 1.7x106 cells, Ang II 2.3x106 cells, PC-61 8.3x105* cells, *P<0.05 vs Con) without changing CD3+ and CD4+ T cell counts. The number of Foxp3+ T cells residing in the kidney was also significantly reduced by PC-61 (Con 1,152 + 368 cells, Ang II 686 + 389 cells, PC-61 210 + 35* cells, *P<0.05 vs Con). Quantitative real-time PCR demonstrated that whole kidney expression of MCP-1 and ENaC alpha were significantly increased in Foxp3+-depleted mice (MCP-1- Con 1.0 + 0.1, Ang II 1.6 + 0.4, PC-61 1.8 + 0.2*; ENaC-α- Con 1.0 + 0.1, Ang II 1.6 + 0.2, PC-61 2.1 + 0.1*, *P<0.05 vs Con). These data suggest that the anti-inflammatory Foxp3+ T regulatory cells play a significant role in mediating the resistance to Ang II hypertension in premenopausal female mice, and may influence renal inflammation and sodium retention during chronic Ang II infusion.

F24

PALMITATE-INDUCED GYLCOSYLATION OF CYCLOOXYGENASE-2 IN PRIMARY HUMAN VASCULAR SMOOTH MUSCLE CELLS. Raman P and Gonzales RJ. Basic Medical Sciences Department, University of Arizona College of Medicine, Phoenix, AZ

Obesity is a major risk factor for cardiovascular health and function. One possible cause of obesity is poor nutrition, including the consumption of diets high in saturated fatty acids. Since vascular inflammation is a key etiological factor in cardiovascular disease, we investigated the effect of saturated fatty acid exposure on the modulation of COX-2 in primary human male brain and aortic vascular smooth muscle cells. Cells were treated chronically (12 to 18 hr) with vehicle (5% BSA and 0.1% ethanol) or palmitate. Protein levels were assessed via western blotting and light microscopy was used to visualize cell density and morphology. Two distinct bands corresponding to the reported 72 and 74 kDa COX-2 glycoforms were detected following palmitate treatment. A dose-dependent increase in both forms was observed with the greatest increase observed in the 74 kDa glycoform (enzymatically active form). Glycosylation inhibition with tunicamycin abolished palmitate-induced increases in the COX-2 glycoforms and augmented band density of a lower migrating non-glycosylated form (64 kDa). Palmitate also increased cell density and altered cell morphology. Although selective COX-2 inhibition with NS-398 further enhanced COX-2 levels in the presence of palmitate, it reversed the palmitate dependent changes in cell density and morphology. In conclusion, this study suggests that palmitate alters COX-2 function potentially by altering its post-translation modification in vascular smooth muscle. This potential novel regulation of COX-2 by saturated fatty acids may contribute as a mechanism in the development of cardiovascular disease in part by altering the structure, function, and health of vascular tissue. *Support: University of Arizona Sarver Heart Center* and *University of Arizona Valley Research Project Grant*

F25

CONTRASTING PROCESSES TO MEASURE MITOCHONDRIAL FUNCTION IN CULTURED MYOTUBES VERSUS WHOLE MUSCLE: PRELIMINARY STUDIES

Ravichandran J, Kras K, and Katsanos CS.
School of Life Sciences and Center for Metabolic and Vascular Biology, Arizona State University and Mayo Clinic, Scottsdale, AZ

Analysis of mitochondrial function is of central importance in understanding the fundamental aspects of cellular energetics. It is particularly important in the case of disorders associated with altered mitochondrial function in muscle. In an effort to delineate effects of environment versus inherent differences in muscle mitochondria function we sought to optimize procedures that measure mitochondria function in muscle samples and primary culture myotubes. Initial optimization steps were done with mouse muscle and cell culture myotubes from human. The muscle solei from mice were permeabilized using saponin (50ug/ml). The muscles were finely teased with scalpel and incubated in saponin buffer I for ~30 minutes. To remove the saponin, the muscles were washed 3 times with buffer II for 15 minutes. Oxygen utilization rates were measured after the washing step with 500uL respiration media. In case of the cell culture, the only difference was a cell count was taken initially and 500,000 cells were used. All preparative procedures were done at 4 ^{O}C. Mitochondrial oxygen utilization responses to substrates such as ADP, Glutamate and cytochrome C were recorded for each of the samples using Hansatech oxygraph with a clark type polarographic oxygen electrode. A preliminary optimization study with permeabilized muscle fibers from mouse and cell culture myotubes from human biopsy yielded respiration rates (nM O_2/min/mg tissue) of -2.62 and -0.23, respectively, with consistent responses among the mitochondrial substrates. Extending these procedures to muscle from healthy and obese subjects and primary cell culture myotubes from these same subjects will provide novel insights into the mechanisms regulating muscle mitochondria function in obesity.

F26

DRUG DISCOVERY: NOVEL PROTEASE ACTIVATED RECEPTOR 2 ANTAGONISTS

Rivas C.M., Hoffman J, Sherwood C, Vagner J, Boitano S
University of Arizona, Tucson, AZ

Protease activated receptor 2 (PAR_2) is a G-protein coupled receptor that possesses the unique ability to self-activate upon proteolysis of the extracellular domain. This event exposes an activating peptide sequence that has guided drug discovery efforts in combating associated inflammatory diseases such as allergic asthma, chronic pain, arthritis and cancer. A primary focus of drug design has been to develop peptides or peptidomemitic ligands that can specifically bind PAR_2 to: 1) invoke full activation in the absence of protease cleavage; 2) invoke full inhibition in the presence of proteolytic cleavage, or; 3) induce biased signaling to best shape physiological response. Recently, our lab discovered the first potent (IC_{50} < 5 μM) full PAR_2 inhibitor, C391 that can block PAR_2-dependent signaling pathways invoked by peptidomimetics or protease agonists *in vitro*, and pain pathway *in vivo*. Using C391 as a template, we initially focused our drug discovery efforts towards developing a bioavailable, low molecular weight potent PAR_2 inhibitor. We tested several smaller, but structurally similar, C391 derivatives for their ability to block PAR_2 dependent signaling. Inhibition is retained, albeit slightly reduced, following removal of the tyrosine moiety from C391. Further shortening combined with alterations in the placement of the 2-furoyl moiety resulted in a loss of antagonistic function. Because lipidation of known PAR_2 agonists has been shown to increase agonist ability ~200 fold, we next tested whether lipidation of C391 could increase antagonism. A lipidated C391 compound decreased IC_{50} to submicromolar values in a Ca^{2+} signaling assay. These initial results provide key structure activity relationships that continue to provide new drug candidates in search of efficacious PAR_2 drugs.

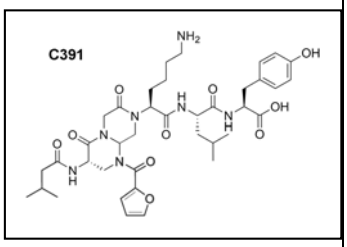

F27

The Kinetics of Ligand Interaction with the Organic Cation NBD-MTMA at OCT2

Philip J. Sandoval and Stephen H. Wright, Department of Physiology, University of Arizona, Tucson AZ

The term "organic cation" (OC) is used to describe a family of structurally diverse organic compounds that are positively charged at physiological pH. It is estimated that 40% of prescribed drugs are OCs that are cleared from the body through a common elimination pathway in the kidney. This process involves two multidrug transporters; OCT2 mediates uptake across the basolateral membrane and MATE1 mediates efflux across the apical membrane. A consequence of OCs sharing these transporters is the potential for adverse drug-interactions. It is of interest to be able to develop predictive models of the selectivity of these transporters in order to prevent unwanted drug-drug interactions. The selectivity of OCT2 has been studied extensively using overexpression systems in cultured cells. To date hundreds of OCT2 inhibitors have been screened against model substrates and the data used to generate predictive models. However, there has yet to be a significant effort to determine the mechanism of ligand interactions with OCT2. By determining the effects of inhibitors on the kinetics of substrate uptake we can determine if substrates interact with a single binding site or multiple binding sites, which is critical for developing accurate models of OCT2. In addition current models do not take into account the presence of unstirred water layers that influence the accuracy of kinetic data and resulting models. In this study we measure the kinetics of inhibition of the fluorescent compound NBD-MTMA at OCT2 against a fixed concentration of the model substrates TEA and metformin. In order to account for the presence of unstirred water layers in our overexpression system we use a mathematical simulation in MATLAB of a uniporter such as OCT2. Our results demonstrate that Metformin and TEA inhibit the uptake of NBD-MTMA by a competitive mechanism. This suggests a single common binding site for these compounds at OCT2.

F28

A POWERED ANKLE-FOOT PROSTHESIS WITH A BIO-INSPIRED CONTROLL ALGORITHM SUCCESSFULLY REPRODUCES HUMAN WALKING AND STAIR ASCENT.

Tahir U, Hessel AL, Petak J, Tester J, Nishikawa KC
Northern Arizona University, Flagstaff, AZ

Advances in prosthesis development have been driven largely by technology (e.g., light-weight materials, long-life lithium batteries, and wireless communication), rather than by advances in our understanding of the underlying biological principles of movement. For a person with a trans-tibial amputation, the iWalk BiOM is a commercially available powered ankle-foot prosthesis that utilizes a motor to assist the user through the gait cycle. Provision of motor power permits faster walking than can be produced using only the spring-like behavior provided by passive devices. The BiOM can adapt to changes in walking speed on level ground, but the use of active motor power raises the issue of control. The main problem is that the control approach exhibits no inherent adaptation to varying environmental conditions. Instead, algorithms are required to generate particular torque control for all intended activities and variations of terrain, along with an appropriate means to select among them. The muscles in our body are able to adapt instantaneously to changes in load without requiring sensory feedback, a property that has remain unexplained for decades. We have developed control algorithms for the BiOM based on the novel winding filament hypothesis (WFH), which builds on the sliding filament theory by incorporating a role for titin. The WFH explains muscle properties including force enhancement and force depression, which are unexplained by the sliding filament theory. We implemented a control algorithm based on the WFH into the BiOM and tested subjects under a variety of conditions including level walking and stair ascent. By implementing a control algorithm that, like muscle, can adapt instantaneously to changes in load, we hope achieve more robust prosthesis control. Our results indicate that the WFH-based control algorithm for the BiOM is capable of producing ankle torque profiles during level walking that are similar to normal human walking. The WFH-based control algorithm is also capable of reproducing ankle torque profiles that match those of able-bodied individuals during stair ascent with no change in parameters. Future studies include metabolic cost of transport, backwards walking, ramp ascent and descent, and walking on uneven terrain such as astro turf and cinders.

Saturday's Abstracts

(Alphabetical, by first author--poster board # shown)

REGULAR MEMBERS

S1

ACUTE EXERCISE ACTIVATES PPARα EXPRESSION AND CARNITINE BIOSYNTHESIS AND UPTAKE IN MOUSE KIDNEY AND LIVER.

Broderick TL, Cusimano FA, Schonert C, Tamura L.
Department of Physiology and College of Osteopathic Medicine, Midwestern University, Glendale, AZ

Fatty acids (FA) are an important source of energy (ATP) during exercise. FA oxidation (FAO) occurs in the mitochondrial and is dependent on carnitine, an obligate factor that transfers FAs from the cytosol into the mitochondria for oxidation and ATP production. Biosynthesis of carnitine occurs predominantly in the liver and is driven by γ-butyrobetaine hydroxylase (BBH), the last and rate-limiting enzyme in the pathway that converts γ-butyrobetaine to carnitine. Carnitine is then released into the plasma and where it is actively taken-up by OCTN2 carriers in contracting oxidative tissues. Since exercise increases FAO, and a high level of FA in plasma during fasting activates peroxisome proliferator-activated receptor α (PPARα) to, in turn, favor the oxidation of FAs, we determined whether exercise increased protein expression of PPARα and if a corresponding increase in BBH and OCTN2 expression in liver and kidney was observed. Swiss Webster mice ran for 1-hour run on a treadmill at moderate intensity. Mice were sacrificed immediately after, and at 4- and 8-hours post exercise. Post exercise plasma FAs were elevated in runners compared to control mice, indicating increased lipolysis. Western blot analysis revealed that PPARα expression in both liver and kidney were increased immediately after exercise. This was associated with an immediate increase in BBH expression in liver and by a delayed (4-h post exercise) increase in the expression of OCTN2 in liver, kidney and heart. Our results indicate that one exercise session increases carnitine biosynthesis and further suggest that uptake in tissues may help dispose of the elevated levels of FAs during recovery. The increase in OCTN2 may also indicate that renal reabsorption mechanisms are active.

S2

SEX DIFFERENCES IN CARDIOVASCULAR RESPONSES TO STRESS IN ADULT RATS PRENATALLY EXPOSED TO DEXAMETHASONE

TM Hale[1], DE Carbone[1], L Madhavpeddi[1], MK Thompson[1], RJ Handa[1,2]
[1]University of Arizona, College of Medicine – Phoenix, [2]Colorado State University

It is well known that even transient prenatal insults can impact cardiovascular function in adulthood. We have hypothesized that adult cardiovascular disease may have its origins *in utero* as a result of exposure to elevated levels of glucocorticoids. In support of this, we have shown that when pregnant rat dams are treated with the glucocorticoid, dexamethasone (DEX), for the last 4 days of gestation, female-specific changes in metabolism, core body temperature, autonomic function, depression-, and anxiety-like behaviors are detected in their adult offspring. The present study investigated the impact of prenatal DEX on arterial pressure and cardiovascular responses to stress in adult male and female offspring. Pregnant dams were administered DEX (0.4mg/kg per day, s.c.) or vehicle on gestation days 18-21. This resulted in a significant reduction in birthweight in DEX-exposed males and females. At 2-3months of age, arterial pressure was assessed via radiotelemetry. Baseline pressures were collected for 3 days in males and for 7 days in females to evaluate blood pressure throughout the estrous cycle (determined by vaginal lavage). In order to assess whether prenatal DEX alters stress-induced hypertensive and tachycardic responses, rats were placed in a restraint tube for 20 minutes, followed by a 2hr recovery period. Restraint-stress testing was performed on diestrus in females. In male rats, prenatal DEX had no impact on arterial pressure under basal conditions or in the elevations that occurred in response to restraint stress. In contrast, the systolic blood pressure in DEX-exposed females was ~10% below that of vehicle-exposed offspring throughout the estrous cycle. No treatment differences were observed in basal diastolic pressure or heart rate. However, prenatal DEX exposure resulted in an exaggerated hypertensive and tachycardic response to restraint stress (Peak percent increases over baseline: SBP: Veh 18% vs. DEX 35%, $p<0.05$; DBP: Veh 20% vs. DEX 50%, $p<0.05$; HR: Veh 20% vs. DEX 56%, $p<0.05$). Moreover, the time to return to baseline pressures and heart rate was longer in female rats prenatally-exposed to DEX. Taken together, these findings reveal sex-specific differences in the prenatal programming of stress-induced hypertension and further support a role for elevated glucocorticoids in development as an origin for cardiovascular disease states in females. Funding: NIH 5 P50 MH082679 and ABRC ADHS14-082990

S3

BODY POSITION EFFECTS ON HEMOLYMPH AND AIR DISTRIBUTION IN INSECTS. J.F. Harrison, M. Duell, J.C. Campbell, A. Kassi, E. Alanis and J.J. Socha. Arizona State University, Tempe.

Gravity is well-known to influence blood distributions and cardiovascular systems in vertebrates, but its effects have received little attention in arthropods. We used synchrotron x-rays at Argonne National Laboratory to visualize the tracheal systems of grasshoppers and beetles. We then quantified the effect of body position on the size of air sacs in different body positions. Insects in the head-up position had expanded air sacs in the head and almost completely compressed air sacs in the abdominal tip, while insects in the head-down position showed the opposite. Anesthesia exacerbated these effects, demonstrating that insects actively resist the effects of gravity. We then used ^{3}H-inulin to measure hemolymph distribution in grasshoppers, and demonstrated that the changes in air sac volumes with body position were associated with, and likely driven by, transfer of hemolymph between body compartments. Our data demonstrate that gravity can drive blood and air flow in insects, and raise questions about how insects and other terrestrial arthropods counteract effects of gravity and cope with changes in center of mass during locomotion. Supported by NSF 0938047.

S4

EFFECTS OF INCREASED PLASMA BRANCHED-CHAIN AMINO ACIDS AND INSULIN ON MUSCLE PROTEIN METABOLISM

Katsanos CS., Tran L., Hoffman N., Dedmon WL., Carroll C.
School of Life Sciences and Center for Metabolic and Vascular Biology, Arizona State University and Mayo Clinic in Arizona, Scottsdale, AZ and Department of Physiology, Midwestern University, Glendale, AZ

Insulin and branched-chain amino acids (BCAA) are two potent stimuli among plasma circulating factors in enhancing muscle protein anabolism. However, little is known whether either BCAA alone or BCAA+insulin enhance muscle protein metabolism in humans. Seven healthy young subjects (gender, 4M/3F; age, 19±1 years; BMI, 23±1) were infused with BCAA (5 umol/kg/min) for six hours (BCAA) and insulin [either 40 mu/m^2/min (n=3) or 80 mu/m^2/min (n=4)] during the last three hours of the BCAA infusion. Another seven (gender, 6M/1F; age, 23±2 years; BMI, 23±1) underwent the same protocol but with saline instead of BCAA infusion (Saline). The effects of BCAA on muscle protein synthesis and whole-body protein breakdown, an indirect estimate of muscle protein breakdown, were studied between BCAA and Saline groups, while those of insulin within each group, and in conjunction with continuous infusion of L-[ring-$^2H_5$]phenylalanine and muscle biopsies at selected time points. There were no differences between BCAA and Saline groups in the fractional synthesis rate (FSR; %/h) of muscle proteins before the insulin infusion (0.06±0.02 vs 0.05±0.01; P>0.05). Insulin infusion did not increase the FSR within either BCAA (0.06±0.02 vs 0.05±0.01; P>0.05) or Saline (0.05±0.01vs 0.06±0.01; P>0.05) groups. However, whole-body protein breakdown (umol/kg/min) tended to be lower in the BCAA vs Saline group (0.97±0.07 vs 1.10±0.05; P=0.09), and decreased following the insulin infusion within both BCAA (0.97±0.07 vs .67±0.3; P<0.01) and Saline (1.10±0.05 vs 0.83±0.03; P<0.01) groups, with a significantly greater effect between groups during insulin (P<0.01). Insulin infusion decreased the concentration of plasma total as well as non-BCAA essential amino acid concentrations in both BCAA and Saline (P<0.05) with no differences between groups (P>0.05). These findings show that the effects of BCAA are augmented by insulin, resulting in suppressed muscle protein breakdown with no changes in muscle protein synthesis.

S5

EVIDENCE FOR PARACELLULAR UREA TRANSPORT IN THE RAT INNER MEDULLARY THIN LIMBS OF HENLE'S LOOPS. K. K. Evans and T.L. Pannabecker. University of Arizona, Tucson, AZ.

Transepithelial solute flows in thin limbs of Henle's loops play critical roles in countercurrent exchange and the urinary concentrating mechanism; our goal is to identify the urea transepithelial transport pathways in these segments.

Tubules were isolated without enzyme digestion and perfused with concentric glass micropipettes by the method of Burg. The lumen-to-bath transepithelial urea flux was determined and permeabilities were calculated.

Urea transport in isolated perfused lower descending thin limbs (DTLs) is not inhibited by peritubular 0.25 mM phloretin or 10 mM ouabain and is unaffected by a 125 mM lumen Na^+ and 0 mM bath Na^+ concentration gradient. The urea flux in upper and lower DTLs is almost completely and reversibly inhibited by peritubular 5 mM lanthanum. Activation energy for transepithelial urea permeability measured at 37° and 16° C in isolated perfused lower DTLs and in ascending thin limbs is approximately 13 kJ/mol, a value that is consistent with channel-like activity.

The data suggest that a substantial fraction of the transepithelial urea flux occurs independently of known facilitated urea transporters such as UT-A1, UT-A2 or UT-A3, is unlikely to be coupled to Na^+ flux and occurs largely by way of the paracellular pathway.

POST DOCS

S6

Structure Studies of Soluble Guanylate Cyclase by Paramagnetic NMR

Cheng-Yu Chen, and William R Montfort
Department of Chemistry and Biochemistry, University of Arizona, Arizona 85721

Soluble guanylate cyclase (sGC) is the primary nitric oxide (NO) receptor and the key enzyme in regulating NO-signaling pathways in mammals. Binding of NO stimulates the production of 3',5'-cyclic guanosine monophosphate (cGMP), which acts as a secondary messenger in regulating physiological functions including vasodilation, platelet aggregation, neurotransmission, and myocardial function. sGC is a heterodimeric heme protein, assembled from two homologous subunits, each comprised of four domains. Although structures of individual domains have been determined by X-ray crystallography or by molecular modelling, very little is known about how these domains assemble into the full-length protein as well as how the binding of NO affects their orientations, which leads to activation of cyclase activity. In past decades, various drugs including YC-1 and Bay-63-2521 have been developed to influence the cyclase activity. Nevertheless, molecular details underlying drug binding are lacking. Paramagnetic NMR including paramagnetic relaxation enhancement (PRE), pseudocontact shifts (PCS) and residual dipolar couplings (RDCs) induced by an unpaired electron provides long distance (10-70 Å) structural information to study multiple domain proteins and large protein complexes. In the following studies, we utilize the iron-heme center of sGC as the paramagnetic metal. Paramagnetic effects are measured by comparing the HSQC spectrum of sGC at different states of the iron-heme upon binding of NO and CO. The differences provide distance and angular restraints from the iron center to the affected protein amides. We have obtained both the native form and the ^{15}N uniform labeled alpha-HNOX domain of sGC. The native form protein has been used to screen crystallization condition and a possible lead condition has been found. The ^{15}N uniform labeled protein will be used to collect HSQC spectrum. The beta subunit containing the iron-heme center has been produced and will be used along with the alpha subunit for paramagnetic NMR studies.

S7

The Role of Gut Microbiota in Cardiac Injury

Danilo, C., Constantopoulos, E., McKee L., Konhilas, J.
University of Arizona, Tucson, AZ

Advances in sequencing and bioinformatics technologies have allowed unprecedented characterization of the gut microbiome. As a result, there is a growing appreciation that our microbial environment plays a critical role in the maintenance of health and the pathogenesis of disease. Accordingly, recent evidence suggests a role for gut microbiota in modulating cardiovascular disease and cardiac injury. We hypothesized that administration of the probiotic, *Bifidobacterium animalis* subsp. *lactis* 420 (B420), to mice will mitigate the pathological impact of ischemic heart disease (IHD), and that anti-inflammatory T regulatory (T_{reg}) immune cells are necessary to impart protection against IHD as a result of B420 administration. Pretreatment with B420 for 14 or 35 days attenuated cardiac injury from ischemia/reperfusion or permanent coronary ligation. Infarcted hearts from B420 treated animals displayed a significant reduction in pro-inflammatory markers and an increase in anti-inflammatory regulatory T cells (T_{reg}). We further show that T_{reg} immune cells are necessary players to communicate this protection by B420 administration. This protection is due, at least in part, to an increase in anti-inflammatory M2 type macrophages in B420 treated animals. These results suggest that administration of the probiotic B420 protects against cardiac injury and that regulatory T cells mediate this effect. Modulation of the inflammatory response by administration of a specific strain of probiotic may offer a rational, safe, and cost effective way to prevent inflammatory damage after cardiac injury.

S8

Genetic and Genomic Response to Selection for Food Consumption in *Drosophila melanogaster*

Garlapow ME, Everett LJ, Zhou S, Gearhart AW, Fay KA, Huang W, Arya GH, Turlapati L, St. Armour G, Hussain YN, McAdams SE, Mackay TFC
North Carolina State University, Raleigh, NC

Food consumption is critical for animal survival. While the role of neuroendocrine feedback loops, food sensing modalities, and physiological state in regulating food intake are increasingly well understood, other genetic mechanisms remain elusive. We applied ten generations of artificial selection for high and low food consumption in replicate populations of *Drosophila melanogaster*. The phenotypic response to selection was highly asymmetric, with efficient selection and an average realized heritability of 0.15 in the lines selected for high food consumption. We assessed correlated responses in body mass and composition; only glycogen content in males was significant. We performed whole genome DNA sequencing of the high and low selection lines, and identified 5,544 single nucleotide polymorphisms (SNPs) within or near 2,081 genes with significantly divergent allele frequencies after accounting for genetic drift. To further nominate candidate genes contributing to response to selection, we evaluated differences in genome wide gene expression between the selection lines using whole-fly RNA sequencing. We identified 1,631 differentially expressed genes in the analysis pooled across sexes, and 1,267 (2,321) differentially expressed genes in females (males). A significant total of 519 genes were both genetically divergent and differentially expressed between the divergent selection lines, among which several have been previously shown to affect food consumption. These genes are excellent candidates for causing the selection response.

S9

A LYMPHEDEMA-INDUCING MUTATION OF CX47, R259C, ALTERS GROWTH PATTERN AND CX43 PROCESSING IN RAT INSULINOMA CELLS

Kanady JD, Pontifex TK, Taylor SZ, Simon AM, Burt JM.
Department of Physiology, University of Arizona, Tucson, AZ.

Connexins (Cx), proteins that mediate direct intercellular communication, are essential for normal vascular development and function. Mutations in Cx47 have been reported to underlie cases of lymphedema in humans, however the cellular and molecular mechanisms responsible for dysfunction have been largely unexplored. This study examines an orthologous mutation in mouse Cx47 to one of these lymphedema-causing mutations, an arginine to cysteine substitution (R259C) in a highly-conserved region of the second extracellular loop. We transfected connexin-deficient rat insulinoma (Rin) cells with wild-type (WT) Cx47 or Cx47R259C either alone or in combination with WT Cx43. Evaluation of cell growth was performed using light microscopy, protein expression through western blot and immunocytochemistry, and electrical coupling via dual whole-cell voltage clamp. Expression of Cx47 in Rin cells resulted in plexiform cell growth. Cx47R259C and Cx43/Cx47R259C coexpressing Rin cells also displayed plexiform growth patterns, but exhibited more elongated gaps between cell groups. Surprisingly, in Cx43/Cx47R259C cells a multiple banding pattern for Cx43 was detected via western blot and full length Cx43 was conspicuously absent. Immunocytochemistry of Cx43/Cx47R259C cells revealed a diffuse cytoplasmic staining pattern for Cx43 and an absence of readily identifiable gap junction plaques. Based on initial electrophysiological recordings, Cx47-expressing Rin cells have a low incidence of electrical coupling. Together, these preliminary data suggest that Cx47 influences cell growth, and subtle alterations in pattern occur with mutation of Cx47 at R259C. Furthermore, Cx47R259C affects cellular processing of Cx43, which may be a potential molecular mechanism by which this orthologous mutation leads to lymphatic defects in humans.

S10

Preliminary computational emulation of a central pattern generator for gait

Authors:
Robert LeMoyne, Christopher Gass, and Kiisa Nishikawa

Abstract:
The neurological foundations for regulating gait are derived from cortical, subcortical, and interneuronal contributions. In particular, the central pattern generator performs considerable control modulation as a function of afferent input. Insight into the central pattern generator from a computational perspective would benefit the understanding of neurological control of gait. We have developed a Matlab program for investigating the state of gait phase, such as swing or stance, based on sensor-derived input, such as through a hall effect sensor. The Matlab program emulates the central pattern generator through a series of sensor-derived thresholds. In accordance to the prescribed sensor thresholds, a gait phase is selected. The Matlab program provides preliminary evaluation of sensor-derived thresholds for the identification of gait status. In addition to a threshold-derived computational algorithm, initial perspective on the utility of machine learning for identifying gait status is provided.

S11

UNIVERSITY OF ARIZONA PHENOTYPING CORE: ADVANCING IN VIVO RESEARCH

Strom J and Granzier H

Genetic engineering of mouse models has greatly advanced our understanding of gene functions and disease states. Due to the pleiotropic effects genes and their temporal expression it is imperative that potential phenotypes are carefully and systematically investigated. The University of Arizona Phenotyping Core serves as a critical resource providing access to state-of-the-art phenotyping equipment and expertise in reliable and innovative phenotyping techniques. The Phenotyping Core specializes in cardiovascular and skeletal muscle research, but also offers a variety of services with broad applicability. For cardiac studies the Core offers services at all levels of phenotyping. *In vitro* services include assessment of contractility and calcium transients in isolated cardiomyocytes and characterization of heart tissue engineered from isolated myocytes or induced pluripotent stem cells. At the level of the whole animal, our *in vivo* services include cardiac function assessment using high fidelity pressure-volume catheters (Scisense) as well as echocardiography (Vevo 2100). In addition, the Core offers radio telemetry (DSI) capable of continuous conscious, unrestrained monitoring of blood pressure, biopotentials (ECG, EMG, etc.), core temperature, and activity. Apart from studying baseline cardiac phenotypes, it is often important to investigate potential phenotypes under pathological conditions in order to gain insight in a gene's effect on disease progression or in the development of potential therapeutics. In order to facilitate this, the Core provides surgical models of cardiac disease including pressure overload (TAC), volume overload (ACF), and myocardial infarction. For skeletal muscle performance and motor coordination, the Core offers grip strength, rota-rod, and hang time tests. Analysis of muscle mechanics is accomplished through the use of the Whole Mouse Test System (Aurora Scientific). This system is capable of assessing muscle mechanics of isolated muscle *in vitro* or *in situ* as well as intact muscle system *in vivo* through the use of a footplate. The Core also utilizes a surgical model of mechanical overload induced skeletal muscle hypertrophy in which ablation of the gastrocnemius results in substantial hypertrophy of the synergistic muscles. In addition, the Core provides a number of exercise paradigms (running wheel, treadmill, and swimming) to serve as acute cardiovascular stressors, assessments of performance, or as tools to study effects of chronic exercise. With these offerings and the expertise in mouse phenotyping, the Phenotyping Core is ideally positioned to assist with and enhance *in vivo* research for a variety of applications.

S12

MYOFASCIAL RELEASE-INDUCED WOUND HEALING IN 3-DIMENSIONAL BIOENGINEERED TENDONS: ROLES FOR FIBROBLAST PROLIFERATION AND COLLAGEN SECRETION

Manal Zein-Hammoud, PhD[1] and Paul R. Standley, PhD[1]
[1]Department of Basic Medical Sciences at the University of Arizona, College of Medicine - Phoenix

Myofascial release (MFR) is one of the most common manual medicine treatments and we recently reported that modeled MFR hastens wound healing in vitro. However, little is known about the mechanisms underlying the efficacy of MFR. Fibroblasts are the principle cell type in fascia, secrete collagen critical to the extracellular matrix and are prime targets for the mechanical strains that MFR imparts. We have previously shown that relatively long duration and low magnitude modeled MFR results in optimal wound healing rates in bioengineered tendons (BETs). The objective of this study is to elucidate the role of fibroblast proliferation and collagen secretion in MFR-induced wound healing.

BETs were cultured on deformable matrices and then wounded using a steel cutting tip. Using vacuum pressure, BETs were uniaxially strained with a modeled MFR stretch magnitude of 3% beyond resting length for 5 minutes using previously published loading and unloading parameters. BETs were then incubated in either 2% fetal bovine serum (FBS; required concentration for fibroblast proliferation) or 0.2% FBS (required concentration to arrest fibroblasts in the G_o phase of the cell cycle). Daily measurements of BETs' width and wound area were recorded over 6 days and quantified microscopically. Human fibroblast collagen staining and nuclei deposition were assessed using colorimetric and immunofluorescence techniques.

Although significant reductions in wound size were observed in nonstrained (NS) and MFR groups cultured with 2% FBS compared to Day 0 (day of wounding), the MFR group displayed significantly improved wound healing versus the NS group (Figure). Both NS and MFR groups showed about 60% reduction in BETs' width at Day 6 compared to Day 0 ($n=11$, $P<0.05$). MFR revealed a 61% increase in collagen staining and more nuclei deposition compared to the NS group at Day 6 ($n=3$, $P\leq0.05$). All measured differences between NS and MFR were completely abrogated when fibroblast proliferative responses were blocked ($n=6$, $P<0.05$).

In conclusion, modeled MFR greatly enhances wound healing rates in BETs. In the absence of fibroblast proliferation, wound healing rates were slowed and collagen secretion was reduced in MFR-strained BETs. If these results are clinically translatable, they support a likely mechanism by which MFR improves wound healing.

UNDERGRADUATES

S13 **EFFECTS OF GENISTEIN DIET ON DIABETIC JEJUNUM FUNCTION AND HISTOLOGY IN THE OB/OB MOUSE**

Altabtabaee, R., Catmull, S., Masood, F., Leung, L, and L. Al-Nakkash. Dept Physiology, AZCOM, Midwestern University, Glendale, AZ.

The ob/ob (leptin- deficient) clinically relevant mouse model was utilized in this study because it mimics the gastrointestinal dysfunction (slowed motility) seen in patients with diabetes. In this study, we examined the effects of genistein diet on jejunum function in female ob/ob and lean mice. We hypothesized that feeding ob/ob mouse a genistein-containing diet for 4-weeks will reverse the slowed intestinal motility by modifying, either, (1) intestinal smooth muscle structure, (2) expression of proteins involved in contractility, (3) the number and distance between contractile events, or, (4) the neurotransmitters involved in contraction. The ob/ob and lean female mice were fed genistein diet (600 mg genistein/kg diet, 600G) for 4 weeks. At the completion of the diet study, mice were euthanized, jejunum was extracted and measures of contractility using a tissue bath system and motility determined using a GIMM video system. Additional segments of jejunum were frozen to run western blot, and morphology assessed using H&E staining and quantification of acetylcholine receptors, AchR, using immunostaining. Tension was measured in isolated segments of jejunum in response to increasing KCl concentrations and there was not any significant difference among the groups. Number of AchR, was significantly less (52%, n=13, $P<0.05$) in ob/ob mice compared to the leans (n=10). In the ob/ob mice, 600G significantly increased (1.5-fold, n=13, $P<0.05$) the number of the AchR. Measurement of total jejunal wall thickness, inner circular (IC) and outer longitudinal (OL) smooth muscle (SM) thickness, and ICSM and OLSM nuclei count was not different in ob/ob and lean mice. Total Sarcoplasmic/Endoplasmic Reticulum Calcium ATPase (SERCA) protein expression in jejunum was (normalized to Actin). SERCA expression was not different in ob/ob females versus leans; however genistein diet decreased SERCA expression in the obese animals by 75%. These data indicate that the slow motility and decreased transit time in diabetic jejunum is likely only due to the decrease of AchR in ob/ob. Supported by awards from: Midwestern University, Soy Health Research Program, and DAREF.

S14 **DOES AN INCREASE IN PLASMA AMINO ACID CONCENTRATIONS STIMULATE SKELETAL MUSCLE PROTEIN SYNTHESIS IN OBESE HUMANS?**

Authors: De Leon, N., Tran, L., Chad C. Carroll, from Department of Physiology, Midwestern University, Glendale, AZ, Hoffman, N., Katsanos, C.

Obesity is a concern for the healthcare community, and current evidence shows that decreased protein synthesis in muscle is a serious consequence of obesity. Therefore, interventions that stimulate protein synthesis are of great importance for obese subjects. Increased plasma amino acid concentrations, can improve protein synthesis by providing the building blocks for proteins and initiating a cascade of molecular events related to the initiation of translation of proteins. However, these events have been studied mostly in healthy individuals. Randomly selected male and female patients were grouped into obese (BMI≥30.0; n=9) and lean (BMI≤25; n=8) categories. Skeletal muscle mixed-muscle protein fractional synthesis rate (FSR) was quantitated using a primed, continuous infusion of L-[2,3,3,4,5,5,5,6,6,6-$^{2}H_{10}$] Leucine. Hyperaminoacidemia was induced in both groups via an infusion of amino acids. FSR was determined using leucine enrichments determined in blood and muscle protein samples. Glucose, insulin, and plasma amino acid concentrations were determined in plasma samples. At baseline muscle protein FSR was lower in lean (lean: 0.080±0.009%·hr^{-1}; obese: 0.060±0.006%·hr^{-1} *P=0.03*), but following hyperaminoacidemia, FSR was normalized (lean: 0.107±0.009%·hr^{-1}; obese: 0.121±0.007%·hr^{-1} *P=0.16*). Change in glucose levels were the same in each group (lean: 5.5±2.5%, obese: 9.6±4.6% *P=0.21*). However, insulin, known to also stimulate muscle protein synthesis, was unexpectedly higher in the obese subjects (*P*=0.04; 2.94±0.80 fold) compared to lean (1.00±0.22 fold). Our results show that plasma amino acids stimulate muscle protein synthesis in obese individuals. However, this effect may be mediated by the amino-acid stimulated greater insulin response. Further research is needed to determine if muscle protein synthesis is stimulated at comparable levels of plasma insulin levels, which would suggest the existence of insulin-resistance to protein metabolism in obesity.

S15 **IS VARIATION IN VERTEBRAL COLUMN MORPHOLOGY ASSOCIATED WITH VARIATION IN AXIAL MUSCULATURE IN KILLIFISHES?**

S. Gillespie, M. Minicozzi and A.C. Gibb

The axial musculature of fishes is characterized by distinctive, "W"-shaped myomeres; however, myomere morphology varies across taxa and little is known about the evolutionary and developmental factors that influence axial morphology. Our long-term goal is to determine if variation in caudal peduncle morphology influences locomotor performance in the killifishes (Cyprinodontiformes). As a first step, we survey axial muscle and vertebral anatomy in the peduncle region of four cyprinodontiform fishes to test the a priori prediction that myomere variation mirrors vertebral column variation. For example, if the neural and hemal spines of the vertebrae form shallower angles (more posteriorly oriented angles) relative to the vertebral column in one species relative to another, then we expect the "W" shaped myomeres will also display shallower angles and form a more compressed "W" shape. We dissected individual myomeres from the axial musculature of the caudal peduncles in Gambusia affinis, Poecilia mexicana, Jordanella floridae and Kryptolebias marmoratus and compared myomere angles to measurements of the vertebral column in cleared and stained individuals. Variation in peduncle morphology is associated with variation in vertebral spine angles: as the neural and hemal spines "bend" toward the posterior vertebral centra (to form a shallower angle), the angle of the anterior cone relative to the vertebral column also decreases. In addition, cyprinodontiform fishes with smaller caudal peduncles appear to have shorter myomeres when normalized to body length. Although there is a point when the sclerotome and myotome separate in development, it is likely that the bony and muscular elements of the axial skeleton are linked developmentally because the vertebrae and axial musculature both form during somitogenesis.

S16 **LOCALIZATION AND DISTRIBUTION OF TRPV4 ON THE LENS EPITHELIUM**

Fernando Ivich (FI), Mohammad Shahidullah, Amritlal Mandal and Nicholas A Delamere. Department of Physiology, University of Arizona, Ina Gittings Building, Rm.101 Tucson, Arizona 85721-0093.

The objective of the present study is to localize TRPV4 on the lens epithelium and determine its distribution in the different regions. Whole rat eyes and isolated lenses are used for this study. Isolation of lenses was done according to published methods from this lab. Eyes or lenses are fixed and paraffin sections prepared and subjected to confocal immunohistochemistry study. Whole eye paraffin sections show TRPV4 staining on the lens epithelium and on the nonpigmented ciliary epithelium. There is some nonspecific staining in the surrounding tissues including equatorial fibers. Diffuse nonspecific staining in the initial sections made it difficult to draw a firm conclusion on the distribution pattern of the protein and its position on the basolateral or apical membrane. Rat lens epithelium appears to express TRPV4 protein on the membrane.

S17

TEMPORAL EXPRESSION OF CYCLOOXYGENSE-2 FOLLOWING MIDLINE FLUID PERCUSSION INJURY IN THE MALE RAT BRAIN.

C Kerrigan[1], P Raman[1], R Rowe[2], J Lifshitz[1,2], and R Gonzales[1], Basic Medical Sciences Department, University of Arizona College of Medicine Phoenix1 and Department of Child Health and Phoenix Children's Hospital[2].

Inflammation is an early response believed to contribute to secondary neuronal degeneration post traumatic brain injury (TBI). Cyclooxygenase-2 (COX-2) is an inducible proinflammatory mediator and is the predominant COX isoform in the brain that catalyzes the conversion of arachidonic acid to prostaglandins. While the inflammatory response is particularly pronounced in the acute phase following TBI, the temporal profile of immune mediators such as COX-2 has not been assessed. Therefore, the objective of the present study was to investigate the time-based protein expression of COX-2 and its associated upstream transcription factor, nuclear factor kappa B (NF□B) in rat brains following experimental diffuse brain injury. Adult male Sprague-Dawley rats were subjected to a midline fluid percussion injury or sham surgery (craniectomy only). Brain-injured rats and uninjured shams were euthanized and whole brain tissue was harvested at 1, 3, 5, 14, 21, and 28 days.. Tissues were homogenized and analyzed for protein content and standard western blotting performed using anti-COX-2 (Cayman Chemical) and anti-NF□B p65 (Santa Cruz Biotechnology). Although COX-2 is typically considered an inducible enzyme, it has been shown to be expressed under basal conditions in the brain. We observed that basal protein levels of both COX-2 and NF□B p65 were present in sham controls. Protein levels of COX-2 were increased following TBI post days 1, 3, and 5. Specifically, two distinct bands corresponding to the reported 72 and 74 kDa COX-2 glycoforms were detected following TBI with the greatest increase observed in the 74 kDa glycoform (enzymatically active form). There were no differences in COX-2 expression 14, 21 and 28 days post-TBI compared to sham. Similar to COX-2, NF□B p65 protein levels were also elevated at earlier time points (days 1 and 3) post-TBI compared to sham. In conclusion, these preliminary studies suggest that the enzymatically active form of COX-2 and its upstream transcriptional regulator, NF□B, may be involved in the acute pathogenic phase of TBI.

S18

HIGH INTENSITY EXERCISE PROTECTS SKELETAL MUSCLE FROM COMPLICATIONS OF DOXORUBICIN TREATMENT

TN Mahmood, AC D'Lugos, C Cosgrave, WL Dedmon, BD Astill, S Patel, M Katsma, R Gonzales, TM Hale, CC Carroll, SS Angadi, and JM Dickinson

Arizona State University, Phoenix, AZ; Midwestern University, Glendale, AZ; University of Arizona, Phoenix, AZ

Doxorubicin (DOX) is a chemotherapeutic agent proven effective for treatment of breast cancer patients; however, it also has devastating side effects that include skeletal muscle wasting and dysfunction. The purpose of this study was to examine the ability of high-intensity interval exercise performed before and during bi-weekly DOX treatments to attenuate adverse effects of the drug on skeletal muscle. We hypothesized that DOX treatment would reduce mammalian target of rapamycin (mTOR) protein kinase activity in skeletal muscle and that exercise would attenuate this response. Eight-week old ovariectomized female Sprague-Dawley rats were randomized to one of four treatments: Exercise+DOX (Ex-DOX); Ex+Vehicle (Ex-Veh), Sedentary+DOX (Sed-DOX); and Sed+Veh (Sed-Veh). DOX (4mg/kg) or Vehicle (saline) intraperitoneal injections were performed bi-weekly for a total of 3 injections (cumulative dose 12mg/kg). Ex animals underwent high intensity (85-95 %VO_2peak) interval exercise (4×4 min bouts) 5d/wk starting 1 week prior to the first injection and continued throughout study duration. Animals were euthanized ~5d following the last injection, during which the soleus and gastrocnemius muscles were dissected and prepped for protein analyses via western blot. Phosphorylated levels of $mTOR^{Ser2448}$ were decreased in both the soleus and gastrocnemius of Sed-DOX ($p<0.05$ vs. Sed-Veh), whereas phosphorylation of mTOR was not altered in skeletal muscle of Ex-DOX. Similarly, there was a tendency for reduced phosphorylation of $4E\text{-}BP1^{Thr37/46}$ in the soleus and $Ulk1^{Ser757}$ in the soleus and gastrocnemius in Sed-DOX ($p=0.1$ vs. Sed-Veh), whereas these levels were unaltered in Ex-Dox. These preliminary data suggest that DOX administration may impact mTOR signaling, and that intense exercise may provide a therapeutic strategy to preserve skeletal muscle mTOR activity during chemotherapy treatment.

S19

DIFFERENTIAL CARDIOVASCULAR AND PENILE RESPONSES TO ANGIOTENSIN II AND BRADYKININ B1-RECEPTOR ANTAGONISM TREATMENT IN SPRAGUE-DAWLEY RATS

McCormick BA[1], Huot-Marchand J-E[2], Carrol CC[3], Carrier S[4], deBlois D[2], Hale TM[11]University of Arizona, College of Medicine – Phoenix, [2]Universite de Montreal, [3]Midwestern University, [4]McGill University.

Angiotensin II (AngII) is a potent growth factor known to promote vascular and cardiac hypertrophy and fibrosis. AngII has also been shown to induce erectile dysfunction although whether this is associated with changes in the cavernosal vascular structure and collagen deposition has not been determined. Moreover, AngII has been shown to regulate bradykinin B1 receptor (B1R) expression in the heart and aorta and concomitant B1R antagonism has been shown to prevent AngII-induced erectile dysfunction. The present study investigated the impact of AngII and B1R antagonism on vascular, left ventricular, and penile tissue remodeling in adult male Sprague-Dawley rats. Rats were treated for 4 weeks with vehicle or AngII in the presence or absence of the B1R antagonist R-954. After treatment, the cross-sectional area (CSA) of the coronary artery, aorta, and the penile dorsal artery were evaluated. Additionally, the left ventricle and the corpora cavernosa were analyzed for collagen content and protein expression. Left ventricular and aortic mass were significantly increased by AngII, and each of these effects were prevented by B1R antagonism. AngII induced a 92% and 34% increase in coronary artery and aortic CSA, respectively. B1R antagonism partially attenuated the coronary artery hypertrophy but had no impact on aortic remodeling. In contrast, there were no significant changes in dorsal artery CSA induced by AngII or B1R antagonism. Collagen levels in the heart were increased by AngII and attenuated by combined B1R antagonism. In contrast, there was no impact of AngII or B1R antagonism on corpora cavernosal collagen deposition. Although Akt and p38 have both been implicated in AngII-induced remodeling and erectile dysfunction, expression of these proteins was not significantly altered in the left ventricle or corpora cavernosa. This study reveals for the first time that AngII-induced mitogenic and fibrogenic responses impact the left ventricle and aorta, but not erectile tissue. Although AngII is known to induce erectile dysfunction, this does not appear to be due to cavernosal artery remodeling or fibrosis.

S20

EVALUATION OF THE VASOPROTECTIVE EFFECTS OF HIGH-INTENSITY EXERCISE PRIOR TO ANTRHACYCLINE CHEMOTHERAPY

O'Neill LM[a], Jarrett CL[a], Crawford M[a], Carroll CC[b], Hale TM[c], Dickinson JM[a], Angadi SS[a], Sweazea KL[a].

[a]Arizona State University, Tempe, AZ: [b]Midwestern University, Glendale, AZ; [c]University of Arizona, Phoenix, AZ

Anthracylines (ACs) such as doxorubicin (DOX) are highly effective chemotherapeutic agents used in the treatment of breast cancer. However, their clinical utility is limited by severe dose-dependent cardiovascular toxicity. In part, ACs are known to induce endothelial dysfunction. Exercise training augments oxidative stress defense mechanisms, and we therefore hypothesized that exercise *preconditioning* would prevent vascular inflammation and normalize expression of endothelial nitric oxide synthase (eNOS). Adult 8-week old, ovariectomized female Sprague-Dawley rats were divided into 4 groups: sedentary + vehicle (Sed+veh) treatment; Sed+DOX; exercise + veh (Ex+veh) treatment; and Ex+DOX. Rats in the exercise groups were *preconditioned* with intermittent high intensity interval exercise training consisting of 4x4 minute bouts of exercise at approximately 85-95% of VO_{2peak} separated by 2 min of active recovery performed 5 days per week. Animals in DOX groups received 4mg/kg of the drug via intraperitoneal injection bi-weekly for a cumulative dose of 12mg/kg. Animals started exercise one week prior to the first injection and continued exercise training throughout. Animals were euthanized 5 days following the last injection. After anesthetization with isoflurane, animals were decapitated, and aortae were isolated for the measurement of total eNOS protein expression through western blot analyses. Contrary to the hypothesis, total eNOS protein expression was not significantly different between Sed+veh and Sed+DOX treated animals ($p>0.05$), and exercise downregulated expression in both Ex+veh and Ex+DOX animals ($p<0.05$). Additional studies are aimed at characterizing expression of phosphorylated eNOS, which may differ from total eNOS as well as the expression of proteins involved in the regulation of oxidative stress and inflammation.

S21

AGE-RELATED DECLINE OF ANOXIA TOLERANCE IN ADULT *DROSOPHILA MELANOGASTER*

James C. Sargent, Jacob B. Campbell, and Jon F. Harrison

School of Life Sciences, Arizona State University Tempe, AZ, 85287-4501

Though much is known about the cause of anoxia in conditions such as heart attack or stroke, we still have a poor understanding of the mechanisms causing cell death and the genetic and physiological processes responsible for variation in survival of anoxia. *Drosophila melanogaster* are particularly interesting models for studying responses to anoxia as they can survive many hours of anoxia and most of their metabolic pathways are identical to those of humans. We hypothesized, based on studies with humans, that younger adults would have a higher anoxia tolerance than older adults. We exposed adult *Drosophila*, ages 1, 3, 5, 7, 9, and 12 days old, to six hours of anoxia. Survival was assessed 24 hours post-treatment; surviving individuals exhibited movement if stimulated. Survival declined with age in a linear fashion for females and in a more exponential fashion for males. Seventy nine percent of adults one day past eclosion survived six hours of anoxia; while only 10% of twelve-day-old adults survived. Additionally, we measured ATP in 1 and 12 day old Drosophila in different durations of anoxia. In anoxia, ATP levels declined rapidly to near-zero levels in both 1 and 12 day old adults. These data show that patterns of gender- and age-associated variation in tolerance to anoxia are similar in Drosophila and mammals, suggesting that Drosophila may be underutilized models for studies of the genetic and biochemical mechanisms of pathology of stroke and heart disease. In addition, based on ATP measurements during anoxia, it appears variation in anoxia tolerance with age is likely attributed to variation in mechanisms relating to anoxia recovery rather than an ability to maintain cellular processes during treatment. This research was partially supported by NSF 1256745 to JFH and the School of Life Sciences Undergraduate Research (SOLUR) Program at Arizona State University, Tempe Campus.

S22

DOXORUBICIN REDUCES PROINFLAMMATORY MEDIATOR EXPRESSION IN BRAIN AND PIAL ARTERIES FROM OVARIECTOMIZED FEMALE RATS. N Vijayavel[1], P Raman[1], C Kerrigan[1], J Echeverria[1], J Dickinson[2], T Hale[1], C Carroll[3], and S Angadi[2,4,5], R Gonzales[1]
[1]Basic Medical Sciences Department, University of Arizona College of Medicine, Phoenix AZ, [2]School of Nutrition and Health Promotion, Arizona State University, Phoenix AZ, [3]Department of Physiology, Midwestern University, Glendale AZ, [4]Department of Internal Medicine, University of Arizona, Phoenix AZ, and [5]Division of Cardiovascular Diseases, Mayo Clinic, Scottsdale AZ.
Doxorubicin (DOX) is a highly effective chemotherapy agent used to reduce reoccurrence and mortality in breast cancer patients. Its use is hampered however owing to severe dose-dependent cardiovascular toxicity in cancer survivors. Multiple mechanisms have been implicated in the pathogenesis of DOX cardiotoxicity, one of which involves inflammation mediated by activation of the NF□B/TLR4/COX-2 pathway. The toxic effects of DOX-induced inflammation in other organ systems such as the brain and vasculature has not been studied. Therefore, we explored the inflammatory potential of DOX by assessing TLR4 and COX-2 levels in cortex and pial arteries isolated from ovariectomized female Sprague-Dawley rats. We hypothesized that DOX would promote inflammation by increasing COX-2 expression along with expression of its upstream innate immune receptor, TLR4, both of which are under the transcriptional regulation of NF□B. Rats were treated with three, bi-weekly, i.p. injections of DOX (4 mg/kg; cumulative dose 12mg/kg) or vehicle (saline) and euthanized 5 days after the last dose. Tissues were isolated, homogenized, and lysates analyzed for COX-2, TLR4 and NFkBp65 protein levels using standard western blotting. Although COX-2 is typically considered an inducible enzyme, it has been shown to be expressed under basal conditions. In brain cortex and pial arteries from vehicle-treated rats, basal levels of COX-2 and TLR4 protein were detected. However, contrary to our hypothesis, levels of COX-2 and TLR4 were decreased following DOX. Cytosolic levels of NF□Bp65 levels were detected in brain and pial vessel lysate, however levels were not altered by DOX. Similar to brain and pial arteries, basal expression of COX-2 and TLR4 were detected in left ventricle and DOX treatment attenuated expression. In conclusion, although others have suggested the involvement of the NF□B pathway during the development and progression of DOX-induced cardiomyopathy, our studies demonstrate a possible novel action for the anticancer agent implicating anti-inflammatory mechanisms, particularly in female cohorts with low circulating levels of gonadal hormones.

S23

Hypermetric Tracheal Scaling as a Factor in Insect Gigantism

Julian Wagner, Meghan Duell, Jillian Ciarlariello, C.J. Klok, Jon Harrison
Arizona State University, Tempe, AZ

In the Paleozoic Era, atmospheric oxygen levels peaked significantly higher than the current level. Along with this oxygen peak came giant insects, many times larger than those currently observed. This suggests that oxygen transport may inhibit insects from becoming giants. If this were the case, then one would expect to observe an increase of investment in gas exchange structures in larger insects, i.e. hypermetric scaling. This has been observed in tenebrionid beetle trachea. In this study, we look at scarab beetles, since they have a large range of sizes including the largest extant insect species. Using sets of micro-CT images of freshly dead scarabs taken at 180 degrees around the beetle, 3d reconstructions of the specimens were made. Using Aviso Fire, the abdominal spiracle and coxal-trochantal areas as well as the femoral tracheal volumes were measured. The spiracle areas showed isometric scaling with a slope of 0.69. The scaling of the area of the coxal-trochantal trachea showed a larger slope than the scaling of the area of the coxa with a p value of 0.09 in a t test. The femur structure showed isometric scaling, whereas the femoral trachea showed hypermetry with a slope of 1.46, which differed from a slope of 1 with a p value of 0.0012 in a t test. These indicate that structures far from oxygen intake at the spiracles scale hypermetrically in scarabs.